Common mycelial network mediated inter-plant signals modulate plant biotic stress responses and defence against foliar pathogens.

Zigmunds Orlovskis[1*], Ēriks Voroņins[1], Annija Kotova[1], Daniels Pugačevskis[1], Kārlis Trevors Blūms[1], Ilva Nakurte[2], Ivars Silamiķelis[1], Soon-Jae Lee[3]

[1] Latvian Biomedical Research and Study Centre, Rātsupītes iela 1k-1, Rīga, LV-1067, Latvia
[2] Institute for Environmental Solutions, "Lidlauks", Priekuļu pagasts, Cēsu novads, LV-4126, Latvia
[3] Department of Ecology and Evolution, University of Lausanne, UNIL-Sorge, CH-1015, Switzerland

***Correspondence:** zigmunds.orlovskis@biomed.lu.lv

Author Orchid IDs:
ZO: 0000-0001-8583-9814
EV: 0009-0004-1644-6864
AK: 0009-0005-8476-516X
DP: 0009-0002-0285-6999
KTB: 0009-0009-5290-3846
IN: 0000-0001-9070-3479
IS: 0000-0002-7932-1047
SJL: 0000-0002-7216-0236

Key words: common mycelial networks, inter-plant signals, plant defence, neighbour modulated susceptibility, systemic signals, pathogen resistance, *Medicago truncatula*, arbuscular mycorrhiza, *Rhizophagus irregularis*, RNA-seq, metabolomics

Summary

- Arbuscular mycorrhizal fungi (AMF) colonize multiple plant hosts and form common mycelial networks (CMNs) that link multiple plants in nature. CMNs are hypothesised to function as a highway for inter-plant information exchange to modulate plant biotic and abiotic stress responses.
- Here we used AMF *Rhizophagus irregularis* to inter-connect two *Medicago truncatula* plants and explored the effect of known plant defence elicitor on pathogen tolerance of AMF-connected inter-plant signal receivers. We analysed *Medicago* leaf metabolites and emitted volatiles together with transcriptome data to compare responses of the inter-plant signal receivers with intact and cut CMN.
- The integrity of CMN significantly affected inter-plant signal receiver responses. Plant defence and signalling pathways were enriched with receiver transcripts that are uniquely changing in the intact vs interrupted CMN along with distinct production of plant isoprenoids – volatile monoterpenes and triterpene saponins. Furthermore, receivers of CMN-mediated signals from stressed senders display

increased resistance to *Fusarium sporotrichoides* and susceptibility to *Botrytis cinerea*.

- Our results highlight CMN contribution to receiver plant responses which may encode susceptibility and resistance factors to different plant pathogens. Future dissection of the mechanisms involved in inter-plant signal decoding will yield novel discoveries on genetic regulation of inter-plant defence priming under pathogen attack.

Introduction

Majority of land plants form symbiotic associations with mycorrhizal fungi (Brundrett & Tedersoo, 2018). Mycorrhizas extend the physiological surface of plant roots and aid nutrient acquisition (Smith & Read, 2010). In addition, mycorrhizal fungi have been demonstrated to enhance plant abiotic stress tolerance (Kumar & Verma, 2018; Bahadur *et al.*, 2019) and induce systemic induced resistance against foliar pathogens (Song *et al.*, 2011, 2013, 2015). This implicates vital ecological roles of mycorrhizas for plant health and nutrition as well as their agricultural importance. Moreover, arbuscular (AMF) and ecto-mycorrhizal fungi are also capable of inter-connecting root systems from multiple plant hosts, effectively forming underground common mycelial networks (CMNs).

The original studies by Francis & Read (1984) and Simard et al., (1997) demonstrated exchange of nutrients between CMN connected trees, sparking exciting debates on "fungal world-wide web" and plant underground "communication" among academics, as well as in media and popular science books. However, further functional studies on inter-plant signals transmitted by CMN other than nutrients have been extremely scarce ever since. In the study by Song *et al.* (2010) infection of 'donor' tomato plants with fungal pathogen *Alternaria solani* induced activity of genes and enzymes involved in plant defences in 'receiver' plants that established CMN with the donors. In another study, Babikova *et al.* (2013) demonstrated the involvement of CMN in modulating headspace volatile profile of naïve pea plants after aphid attack on their neighbours. CMN is therefore hypothesised to function as information superhighway in transferring diverse signals from plant-to-plant in response to biotic stress stimuli (Bais *et al.*, 2004; Barto *et al.*, 2012). Nevertheless, the nature of CMN-mediated plant alarm signals remains uncharacterised. Similarly, the genetic mechanisms encoding inter-plant signals in senders and decoding in CMN-connected the responders have not been yet described experimentally.

In nature plants are known to engage in both "wired" (via CMN or parasitic plants) and "wireless" (via headspace or root exudates) exchange infochemicals, as reviewed in Sharifi & Ryu (2020). Therefore, many inter-plant signals likely occur together and interact with each other. Paramount to understanding the role of CMN in ecological interactions include experiments where CMN can be interrupted whilst other "wireless" signals remain untampered. For example, in the experiments by Song *et al.*, (2010), tomato plants were bagged to prevent plant exchange by volatile compounds and enable only root-to-root signals, thus limiting the interactions between CMN and volatile signals. We wished to test the hypothesis whether CMN mediates inter-plant signals by characterising the transcriptional and metabolic

responses of signal receiver plants that eavesdrop on their neighbours, and use careful manipulation only of CMN continuity in the background of uninterrupted exchange of headspace volatiles and root exudates.

To this end, we used model AMF *Rhizophagus irregularis* to establish CMN between two *Medicago truncatula* plants, then subjected the leaves of signal senders to known plant defence elicitors and analysed leaf responses in naïve signal receiver plants. Surprisingly, we identified CMN-dependent transcriptional changes in receivers which involve modulation of plant biotic stress responses. Moreover, after the elicitation of sender plants, the CMN-connected receivers displayed increased susceptibility to fungal pathogen *Botrytis cinerea* and increased resistance to *Fusarium sporotrichoides*.

Materials and Methods

Plant growth

Medicago truncatula R108 seeds were scarified and germinated on wet filter paper for 2-3 days, then planted into 1L pots with autoclaved soil:sand (3:1 v/v) mixture. Each pot used for RNA-seq and pathogen experiments contained two seedlings, each placed in a 30 µm autoclavable PA6-grade nylon mesh pocket (JPP140 from Technical textiles, Ekobalta, Latvia). Soil was purchased from Biolan Baltic OÜ (pH: 6,0; EC: 25 mS/m; N~100 mg/L; P~60 mg/L; K~200 mg/L; peat fraction<20mm), kvarz sand had grain size 0-0.5mm and obtained from SACRET®, Latvia. Plants were grown in growth cabinet (SANYO MLR-351H, Japan) at 20□, 50%RH, 16h day / 8h night cycle using a mixture of 6500K and 2700K fluorescent lightbulbs (T8 MASTER TLD G13 Philips, 36W, 3200lm) to cover the entire PAR spectrum and emit ~ 300 mmol m^2 s^{-1} light intensity. Plants were watered with aprox. 200mL of 0.5X Hoagland nutrient solution per pot once per week.

AMF cultivation & inoculation

Rhizophagus irregularis (DAOM 197198) was cultivated on *Daucus carrota* hairy root cultures (St-Arnaud *et al.*, 1996; Baranski, 2008; Ron *et al.*, 2014), grown on M-media (1% sucrose, 0.4% Gelrite gellan gum) at 25□ in darkness. 6-month old cultures were processed for *R. irregularis* spore collection using 10mM citrate buffer (pH=6) to dissolve spore-containing solid media and capture spores within 40µm cell stainer (SPL Lifesciences) and resuspend in sterile water. Suspension with 200 spores was applied to one of the seedlings in the pot. Plants were grown for 7 weeks to establish CMN between the sender and receiver plants. The colonization status of the receiver plant was verified using ink-vinegar staining method (Vierheilig *et al.*, 1998) after the experiment.

Treatment of CMN and sender plants

7-weeks post inoculation all experimental pots were divided into two groups: 1) uninterrupted CMN (sender-receiver plants remain connected via CMN) where a blunt knife was inserted into the soil along the edge of the pot as a control and 2) a group of cut CMN where a blunt knife was inserted into the soil between the mesh pockets to disrupt the CMN connection between signal sender and receiver plants. 3d

after this manipulation mechanical wounding (3x squeezes with forceps) and a 5 µL drop of µM bacterial flagellin (*flg22*, MedChemExpress, Sweden) was applied to two fully expanded trifoliate leaves of the sender plants. 5 µL of water without mechanical wounding was used as control. Receiver plants were left untreated and collected 3 days after the stimulation of the sender plants.

RNA extraction & transcriptome sequencing

Three separate trifoliate leaves from 8-weeks old receiver plants were harvested in liquid N_2, homogenized with pestle and mortar for RNA extraction using ReliaPrep™ RNA Miniprep System (Promega, cat. Z6012). RNA quantification was performed with Qubit™ RNA BR Assay Kit and Agilent Bioanalyzer RNA 6000 Pico Kit. Samples from 4 different plants were processed as biological replicates for each treatment. Total 400ng of each RNA sample (RIN≥7, $OD_{260/280}$ between 1.9-2.1, $OD_{260/230}$ between 1.5-2.0) was processed for library preparation using MGIEasy RNA Directional Library Prep Set following manufacturer's instructions. QIAseq FastSelect –rRNA Plant Kit (QIAGEN) was used to deplete rRNA prior to the library fragmentation step. Qubit® dsDNA HS Assay and Agilent HS DNA Kit was used to determine library concentration and length (average 326 nt) prior to multiplexing and circularization. The final pooled libraries (1.94 ng/µL) were sequenced on DNB G400RS high throughput sequencing machine (MGI) using FLC PE150 flowcell.

Raw data processing and DEG analysis

Read filtering and adapter removal was performed with *fastp 0.20.0* (default parameters; read trimming >100 bp). *STAR 2.7.10a* (Dobin & Gingeras, 2015) was used to map the reads against *Medicago truncatula R108* reference genome available in https://medicago.toulouse.inrae.fr/MtrunR108_HiC (INRA, Toulouse). *SortMeRNA version 4.3.6* (Kopylova *et al.*, 2012) was used to quantify and filter rRNS using smr_v4.3_default_db database. DEG analysis was performed with *limma* (Bioconductor) (Ritchie *et al.*, 2015).

Functional enrichment analysis

Enrichment of GO biological and molecular functions for DEGs was calculated using *agriGO v2.0* (Tian *et al.*, 2017) Fisher exact test (FDR) with *MtrunR108_HiC_functional annotation* file as reference and visualized with enrichment bubble *SRplots*. Additional gene function predictions were performed with *Mercator4 v2.0* (Lohse *et al.*, 2014), based on plant gene orthology search for *MtrunR108_HiC.1.0.fasta_features* as input. Visualisation of differentially regulated gene functions was performed with *MapMan v3.7* (Thimm *et al.*, 2004) and *PageMan* (Usadel *et al.*, 2006) functional annotation tools. The graphical overview of plant defence pathways displayed in **Fig. 2** was drawn manually and loaded as separate pathway image file into *MapMan* (available in **Figure supplement 6**). The mapping file listing gene identifiers and descriptions for the manually assigned functional bins is available in **Supplementary Table 2.** Statistical analysis on DEG enrichment for *MapMan* pathways was performed using built-in Wilcoxon rank test and Benjamini-Hochberg (BH) p-value correction (Usadel *et al.*, 2005).

Correlation of gene expression and metabolite data

Regularized canonical correspondence analysis (rCCA) was used with the *mixOmics* R package (available from Bioconductor; http://www.mixOmics.org) in R studio. R script provided in **Supplementary Table 4 tab D.** Correlations >0.7 were visualised via *Cytoscape* v3.10.3.

rt-qPCR

M. truncatula gene specific primers were designed in NCBI Primer BLAST based on homologous sequences of *A. thaliana* immunity genes. MtTUB was used as the reference. cDNA was synthesised with *Maxima First Strand cDNA Synthesis Kit (Thermo Fisher Scientific)* and qPCR performed with *Maxima SYBR Green/ROX qPCR Master Mix (2X) (Thermo Fisher Scientific)* on *ViiA™ 7 Real-Time PCR System (Applied Biosystems)* and analyzed with the native *QuantStudio 7 Pro 1.6.1* software.

Leaf metabolic analysis with LC-HRMS

Metabolome was analysed from the same leaf samples as plant transcriptome by aliquoting 200mg of the frozen homogenized leaf tissues and resuspending in 1.5 mL of 70% methanol, vortexed for 1 minute and left for maceration for 5 days in a cool, dark place. The obtained extract was filtered through a 0.45 µm filter and injected into the Agilent 1290 Infinity II series HPLC system combined with Agilent 6530 qTOF MS system (Agilent Technologies, Deutschland GmbH, Waldbronn, Germany). Zorbax Eclipse Plus C18 Rapid Resolution HD (2.1×150mm, 1.8µm particle size) column was used at a flow rate of 0.3 mL/min. The column oven was set at 45°C, and the sample injection volume was 3 µL with 40 sec needle wash (70% methanol). The mobile phase consisted of a combination of A (0.1% formic acid in water) and B (0.1% formic acid in acetonitrile). Gradient elution program was used as follows: Initial 5%B, 0-6 min 20%B, 6-20 min 40%B, 20-23 min 80%B, 23-28 min 95%B, 28-33 min 95%B, 33-39 min 5%B. UV/VIS spectra were recorded at 280 nm and 330 nm. The adjusted operating parameters of the mass spectrometer were set as follows: Fragmentation: 70 V; Gas temp: 325°C; Drying gas 10 L/min; Nebulizer 20 psi; Sheath gas temp 400°C; Sheath gas flow 12 L/min. Electrospray ionization (ESI) was used as a source in operating in positive mode. The internal reference masses of 121.050873 m/z and 922.009798 m/z (G1969-85001 ES-TOF Reference Mass Solution Kit, Agilent Technologies & Supelco) were used for all analyses of the samples. The Agilent MassHunter Qualitative analysis 10.0 data acquisition software was applied to analyze LCMS data and compare ion fragmentation data with information available in literature and databases, such as METLIN, LIPID MAPS®, Phenol – Explorer, Lotus - Natural Products Online and FooDB Version 1.0.

Plant Volatile analysis

12h prior to sample collection for RNA-seq and metabolome analysis, a trifoliate leaf from the receiver plant was inserted into clean 20 mL headspace vials for overnight volatile capture whilst still attached to the plant. Upon sampling the leaves were detached, vials were capped and weighed. The fresh plant samples were heated in an incubator before injected into Agilent Technologies 7820A gas

chromatograph coupled with an Agilent 5977B mass selective detector (MSD) using a Gerstel MPS Autosampler. A polar CP-Wax 52CB capillary column (50 m × 0.32 mm, 0.20 µm film thickness) with polyethylene glycol was employed. Helium (He) was used as the carrier gas with a split ratio of 1:20 and a flow rate of 1.2 mL/min. The incubation temperature was set at 125°C for 40 minutes, with an agitator cycle of 30s on and 15s off. The syringe temperature was 130°C, and the injection volume was 2500µL. The temperature program started at 60°C, increased at a rate of 10°C/min to 250°C, and was held for 3 minutes. The injector temperature was 260°C. Mass spectra were recorded at 70 eV within the m/z range of 50-500. The ion source temperature was maintained at 230°C. Compound identification relied on retention indices (determined using a homologous series of C5–C24 n-alkanes) and comparison of mass spectra with the NIST (National Institute of Standards and Technology) MS search 2.2 library. Agilent MassHunter Qualitative Analysis 10.0 data acquisition software was used for HS-GC-MS data analysis.

Plant pathogen assays

Fusarium sporotrichoides (Fs) and *Botrytis cinerea (Bc)* were grown on 0.5X PDA at 20°C in darkness for 4 weeks. Mycelial plugs, obtained with a 7.5mm diam. cork borer, were placed on three different trifoliate leaves. Each leaf was placed in a 5.5cm diam. Petri dish with moist filter paper to maintain high moisture level. The edge of the petri dish had a pre-cut slit for the leaf petiole to remain attached to the plant throughout the experiment. Plants were placed in a shaded place at 20°C for 72h. Agar plugs were removed before leaf photography. *ImageJ (Fiji)* was used to measure the area of necrotic lesions, chlorotic zones (*Bc*) and expansion of *Fs* aeral mycelium.

Results

Wounding combined with flg22 induces local leaf responses and systemic acquired resistance to Botrytis cinerea

Before setting-up experiments with inter-plant signal senders and receivers, we first wished to perform preliminary experiments to select leaf stimuli that would trigger gene expression changes in *Medicago truncatula* and display altered plant response to a pathogen. To this end we decided to test mechanical wounding by forceps as well as a well-known plant immunity elicitor - bacterial flagellin (*flg22*). Since *flg22* and wounding have been well documented to induce different defence responses in leaves of a model plant *Arabidopsis thaliana* (Pieterse *et al.*, 2009) and are required in combination to activate defence in plant roots (Zhou *et al.*, 2020), we also decided to test the combination of both stimuli which would mimic a natural scenario where bacterial infections follow mechanical plant damage. While the application of chemical elicitors and wounding by forceps can be expected to be easily controlled and highly reproducible in complex follow-up experiments, we also decided to infiltrate a mixture of live plant pathogenic bacteria with a broad host range (*Pantotea aglomerans, Pseudomonas syringae pv. tomato, Erwinia rhapontici, Dickeria chrysanthemi*) to test for their ability to trigger local responses in the infected leaves. We selected a range of known plant immunity genes as potential

markers for local leaf responses, designed primers for their homologs in *Medicago* and performed rt-qPCR at 2h, 4h and 6h following the application of stimuli. Leaves infiltrated with *flg22* and leaves treated with the combination wounding and *flg22* (*w+f*) displayed strong induction of *MtPAD4* already at 2h, while *MtVSP1* expression was strongly induced at 4h and 6h following *w+f* treatment (**Supplemental Figure 1**).

Next, we tested the performance of fungal pathogen *Botrytis cinerea* on distal (systemic) leaves of *Medicago truncatula* 24h after stimulation of the local leaves. The *w+f* treatment reduced the area of necrotic zones under *Botrytis* inoculation site compared to water controls, characteristic of systemic acquired resistance (SAR) (**Supplemental Figure 2**). Together with marker gene expression data, mechanical wounding combined with flagellin application appeared to produce early local leaf responses as well as systemic responses that contribute to altered pathogen performance in our experimental system. Therefore, this treatment was chosen as a sender plant trigger for evaluating receiver plant responses in the following experiments.

CMN mediates receiver plant responses to stimulation of signal senders

We placed two *Medicago truncatula* seedlings in a single pot. Each plant was grown in a separate 30 µm nylon mesh pocket that permits extension of AMF hyphae and plant root exudates but prevents direct physical contact of the plant roots. We inoculated one of the plants with *Rhizophagus irregularis* and grew for 8 weeks to establish CMN. We then used a blunt knife to cut the CMN between the plants (**Figure 1A**; treatment ‘’cut’’). To leave CMN intact but control for the effect of physically touching or wounding the AMF mycelium, we placed the knife within the far edge of the other pot (**Figure 1A**; treatment ‘’connected’’). This way we avoid the potential confounding effect of plant responses to wounded AMF hyphae and truly can test effect of the continuity of CMN as opposed to the cutting or rotating of nylon mesh pockets done in previous studies before. The nylon mesh pockets also protect plant roots from accidental wounding during the CMN cutting treatment. Next, we stimulated the sender plants with mechanical wounding and *flg22* treatment or applied water for control (**Figure 1A).** 3 days after the stimulation, we harvested the leaves of receiver plants for whole transcriptome sequencing.

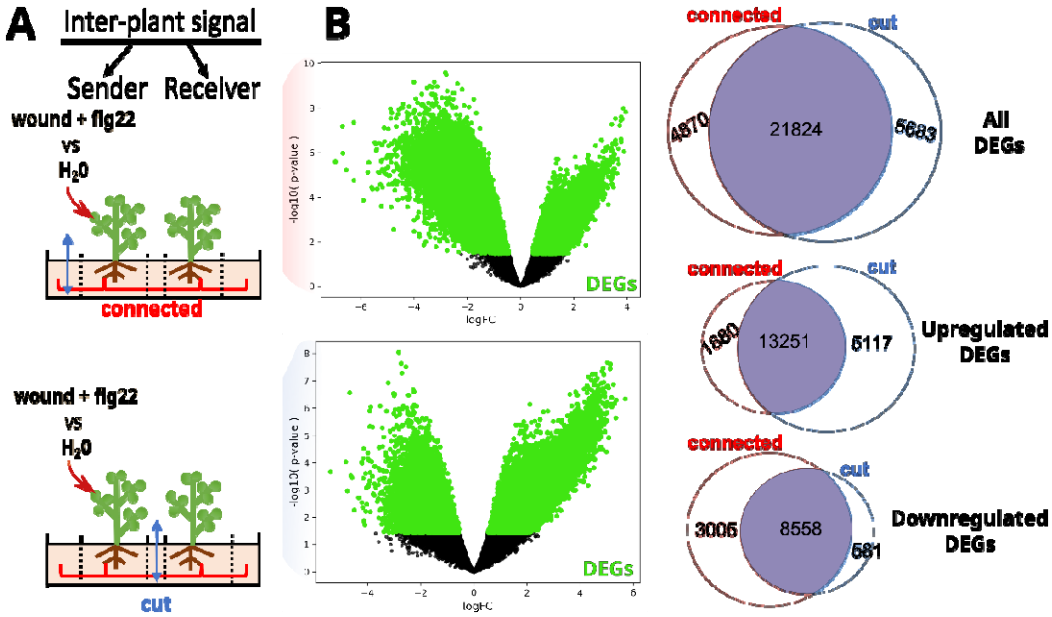

Figure 1. Intact CMN contributes to wound and flagellin induced inter-plant responses. (A) A duet of *Medicago* plants were grown in 30 µm mesh pockets (dashed lines) and inoculated with AMF *Rhizophagus iregularis* to form CMN (red). Position of knife insertion is indicated with a blue double-head arrow. Sender plants of the cut-CMN and the intact-CMN pots were stimulated by wounding and *flg22* application to measure responses in the receiver plant leaves. **(B)** Wounded and *flg22 (w+f)* treated plants were compared to H_2O to identify up- and down-regulated responder plant DEGs in the intact-CMN pots (red circles) and the cut-CMN (blue circles). Volcano plot displays log10 of p-adj. and log2 of fold change for each transcript in the *(w+f)* comparison with water controls. Each treatment contained 4 replicate plants.

We found that naïve receiver plants display strong transcriptional responses to leaf wounding and *flg22* application on their neighbouring sender plants. We identified around 27.5 thousand DEGs in the cut-CMN and 26.7 thousand DEGs in the intact-CMN treatments (**Figure 1B**), suggesting a potential strong contribution of headspace volatiles and exudates in inter-plant responses. Nevertheless, when we compared the responses from receivers that were either cut-off or connected to their senders via CMN, we identified 1880 up- and 3005 down-regulated DEGs that characterise receiver responses dependent on the intact CMN (**Figure 1B**). Among those were 15 DEGs that showed opposite regulation in the cut-CMN and the intact-CMN treatments. Crucially, we also wished to test the effect of touching and cutting AMF hyphae on plant responses. Surprisingly, when we compare receiver responses to water treated senders in cut-CMN and intact-CMN, we observed not a single DEG (**Supplementary Figure 3**). This strongly indicates that the CMN cutting was done evenly across all treatments and supports our finding that intact CMN contributes to unique inter-plant responses to sender stimulation with wounding and *flg22*.

CMN-dependent inter-plant signals involve transcriptional modulation of plant defences

Next, we wished to characterise the functions of the 1880 up- and 3005 down-regulated responder plant DEGs that change in response to stimuli from sender plants

only with intact-CMN. To this end, we used *AgriGO v2.0* for functional enrichment and visualisation of linked gene GO annotations. Interestingly, only 2 biological functions - DNA integration and DNA metabolic process – were significantly enriched with the 1880 upregulated DEGs (**Supplemental Figure 4A; Supplemental Table 1 tab-A**). In contrary, 302 different biological process, molecular function and cell compartment associated GO-terms were significantly enriched with the 3005 downregulated DEGs (**Supplemental Table 1 tab-B**). Functions with the most significant enrichment of downregulated DEGs relate to ribosome structure and RNA binding (**Supplemental Figure 5A).** Intriguingly, when we manually examined the GO function list, we noticed a series of individual GO-terms related to plant stress responses such as metabolism of ROS, response to stimuli and jasmonic acid (**Supplemental Table 1 tab-B**). These GO-terms appear to constitute a cluster of functionally linked stress response categories and displays higher DEG enrichment factor (**Supplemental Figure 5B)** compared to other more generic GO-terms (**Supplemental Figure 5C).**

When we searched for the representation of assigned GO functions within *M. truncatula* R108 annotated reference genome, we found that 31'310 out of total 39'027 genes (80.22%) had assigned GO annotations. Furthermore, 83.86% or 4083 genes from the 4885 DEG list had functional annotations available (**Supplemental Table 1 tab-C**). Together, this suggests that we obtained reasonably large and representative functional enrichment estimate.

Nevertheless, to complement our approach thus far, we wished to perform and an independent function inference and enrichment. Therefore, we additionally submitted all genomic *Medicago truncatula R108* mRNA FASTA sequences to *Mercator4* tool (Lohse *et al.*, 2014) for homology-based *de novo* function predictions based on annotated plant orthologs and generate a reference gene function mapping file (available as **Supplemental Table 2 tab-A**). We then supplemented GO-term enrichment with *Mercator4* functional bins. For the upregulated DEGs, phosphotransferase activity and protein modifications appear to accompany DNA integration and DNA metabolic process enrichment (**Supplemental Figure 4B**). For the downregulated DEGs, the *Mercator4* functions were largely congruent with the GO-term enrichment in highlighting the ribosomal subunit organization, RNA processing, translation as well as responses to jasmonic acid (**Supplemental Figure 5C**).

When we manually inspected the annotations and bin structure obtained in our *de novo* functional predictions, we noticed that many known biotic stress related functions are ordered under different pre-existing bins rather than organized together as one (**Supplemental Table 2 tab-B**), potentially underscoring the DEG enrichment for biotic stress responses. 16.9% of all genomic *M. truncatula* transcripts could be assigned to defence-related functions (**Supplemental Table 2 tab-C**). Since we found many stress response related GO-terms enriched with downregulated DEGs in our previous analysis steps, we took a similar approach to the recent study in *Arabidopsis* (Orlovskis *et al.*, 2024) and manually curated a novel ''Defence signalling & response'' bin previously absent from the *Mercator4* annotation (**Supplemental Table 2 tab-D**). We then compared the cumulative fold change of receiver plant transcripts across different functional categories for better assessment of biotic stress

responses using *PageMan* and *MapMan* tools (Thimm *et al.*, 2004; Usadel *et al.*, 2006).

Interestingly, the ''Defence signalling & response'' category displayed one of the strongest wounding and flagellin induced inter-plant responses (alongside protein biosynthesis and photosynthesis) in receivers with intact CMN (**Supplemental Table 3 tab-A**). Concomitantly, these biological functions contained the highest cumulative transcript fold change of the 4885 DEGs for the intact-CMN compared to the 5683 DEGs specific to cut-CMN treatment (**Figure 2A**). Furthermore, visualisation of the manually curated defence signalling & response pathway, highlights downregulation of enzymes involved in ROS homeostasis, receptor-like kinases and intracellular MAP and Ca-dependent kinases, as well as Ub-proteasome pathway (**Figure 2B; Supplemental Table 3 tab-B**). Notably, inter-plant signals had modulated transcripts of cell wall enzymes and triggered downregulation of genes involved in jasmonic acid synthesis and perception more than salicylic acid pathway. However, surprisingly, receiver plants did not display abundant transcriptional changes in genes encoding specialized metabolites, except terpenoid and flavonoid synthesis.

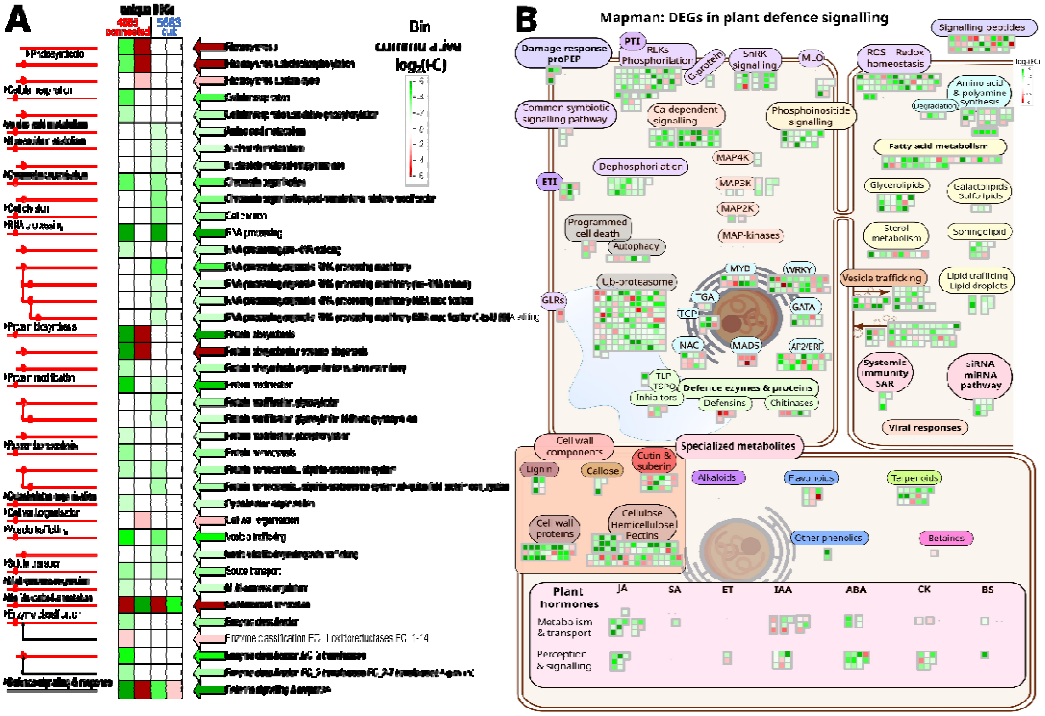

Figure 2. Intact CMN mediates remodelling of biotic stress responses in inter-plant signal receivers. (A) Cumulative transcript fold changes of plant functions encoded by up- and down-regulated DEGs which are specific to either intact CMN treatment or cut CMN treatment do not overlap and are different. Visualisation was based on *Mercator4* functional annotation via *PageMan*. (**B**) 884 DEGs corresponding to plant biotic stress responses and plant defence signalling display dramatic transcriptional responses in responders with intact CMN. Green colour represents downregulated, red – upregulated DEGs with colour intensity proportional to log2FC. Genes are assigned to immune receptors, intra-cellular signalling components and other defence related functions as indicated in **Supplemental Table 2.** Full list of DEGs, their annotation and individual fold-changes displayed here are provided in full

in **Supplemental Table 3 tab-B.** The image file for MapMan visualisation of ''Defence signalling & response'' pathways is available for download as **Supplemental figure 6.**

Inter-plant signals modulate plant volatile and metabolite composition in CMN-dependent manner

In the study by Babikova & colleagues (2013) pea receiver plants which were connected to aphid infested donor plants displayed altered volatile production. Therefore, we wished to further analyse leaf metabolites and headspace volatiles using untargeted metabolomics approach. Leaf samples for metabolomics were collected simultaneously with the samples for RNA-seq from the same plants, enabling comparison and correlation of both datasets. When *Medicago* senders were wounded and treated with *flg22* (**Figure 3A**), CMN-connected responders display significantly reduced production of volatile leucinamide (V2) and increased production of monoterpenoid β-fenchyl alcohol (V5) alongside several other leaf compounds such as medicagenic acids (L45; L47), acetylsoyasaponin (L46), genistein 7-O-glucoside (L15), 1H-Indole-3-acetaldehyde (L3), tyrosine (L8) and hex-bayogenin (L42) when compared to signals from H_2O treated senders (**Figure 3B**). Notably, these compounds were not significantly over- or under-produced in inter-plant signal receivers with the interrupted CMN, suggesting CMN-dependent metabolic changes to neighbour signals. Instead, leaf metabolites soyasapogenol E (L51) and proline (L9) were significantly upregulated while mannopyranoside compound (L52), chrysoeriol (L19) and tricin GlcAGlcA (L20) were downregulated in receivers with cut CMN (**Figure 3B**). Interestingly, receivers with the interrupted CMN did not show significant increase or decrease in volatile production unlike receivers with the intact CMN.

Given these differences, we further wished to identify compounds which displayed the greatest relative differences in inter-plant signal responses between the interrupted and intact CMN. We identified a group of volatile compounds which showed decreased production in receivers with cut CMN but not with intact CMN (**Figure 3C,** Cluster1), including several monoterpenoids linalool oxide (V8), myrcene (V3) and carotenoid derived aromatic ketones – ionone (V23) and its furan derivative (V23). Interestingly, biotic stress is known to induce production of linalool which increased H_2O_2 and intracellular Ca^{2+} concentrations in mesophyll cells (Jiao *et al.*, 2022). Linalool is often converted into pyranoid and furanoid linalool oxides and involved in pollinator and herbivore attraction (Raguso & Pichersky, 1999). Linalool is positively regulated by MYC transcription factor and confers resistance to phytopathogenic *Pseudomonas* in lavender (Dong *et al.*, 2024). Terpenes such as myrcene are insect pest deterrents (Boncan *et al.*, 2020) and their production is induced by mycorrhization, suggesting a mechanism how CMN may aid plant defence against herbivores and alert neighbouring plants via terpenoid production (reviewed in Sharma *et al.*, 2017). Interestingly, ionone produced by tomatoes induced resistance against flower trips (Murata *et al.*, 2020) and has also been shown to mediate inter-plant defence priming against *Blumeria* infection in barley (Brambilla *et al.*, 2022).

Furthermore, another set of metabolites showed the opposite trend – decreased production in receivers with intact CMN but no or weak response to wounding and *flg22* in receivers with cut CMN (**Figure 3C,** Cluster2). These included plant volatiles

leucinamide (V2), ferulic acid derivative 4-vinylguaiacol (V27) and isoprenoid compounds - mesitylbuta-1,3-diene (V21), dihydrodehydro-β-ionone (V25), thujone (V17) - as well as urea (V7) and methylurea (V9). While there is no documented direct link between leucinamed and plant defences, amides such as hydroxycinnamic acid (Liu *et al.*, 2022) and polyamides (Yi *et al.*, 2024) play important roles in plant immunity. Ferulic acid and its bioconversion products such as 4-vinylguaiacol are involved in cell wall strengthening and exhibit antioxidant and antimicrobial properties (Tanruean & Rakariyatham, 2014; Antonopoulou *et al.*, 2022). Thujone derives from monoterpenoid sabinene and is associated with inhibitory activity against phytopathogenic fungi (Bai *et al.*, 2020) as well as reduced herbivore damage (Gesell *et al.*, 2015) in gymnosperms.

Given that many isoprenoids, in particular monoterpenes, appear to be differentially produced in cut and connected CMN receivers (**Fig. 3C)**, we searched for KEGG monoterpenoid pathway gene homologs in *M. trucatula* genome to display receiver plant gene expression in response to sender signals. Surprisingly, myrcene, linalool and sabinene synthesis genes were higher upregulated in responders with cut CMN compared to intact CMN but oxilinalool synthesis gene was more downregulated in responders with intact CMN compared to cut CMN, which is opposite to the measured metabolite tendencies (**Supplemental Figure 7**). While this may be linked to negative feedbacks on gene regulation, we wished take an unbiased view and search for the strongest correlation between changes in gene expression and metabolite production. To this end, we took the set of 4885 DEGs specific to wounding and *flg22* response in receivers with intact CMN and performed regularized canonical correspondence analysis (rCCA) to display correlation network between metabolite production and the associated gene expression. Surprisingly, proline (L5) and soyasapogenol E (L51) displayed strong correlation with a number of genes involved in plant defence responses (**Figure 3D),** including plant surface LRR Ser/Thr kinase receptors, including the flagellin receptor *FLS2*, *PATHOGENESIS RELATED 4*, E3 Ub ligases PUB22 and PUB23, ethylene and gibberellin response factors as well as several transcription factor families, especially MYB-related and GRAS. Interestingly, aquaporin gene *NIP2* expression was strongly associated with ethyl-d-gluccopiranoside (L9) and HO-α-muurolene (V24) (**Figure 3D).**

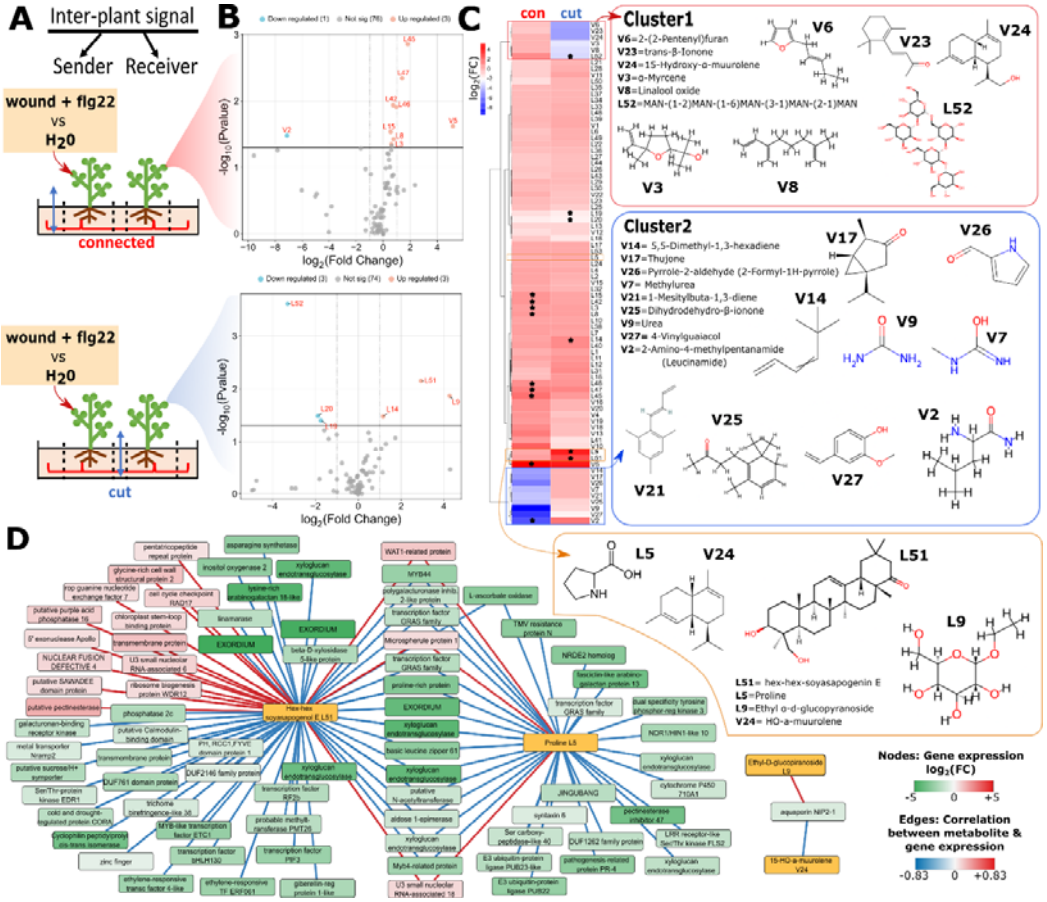

Figure 3. CMN modulates leaf metabolite and volatile production in response to neighbour stress-induced signals. (A) Two *Medicago* plants were grown in 30 µm mesh pockets (dashed lines) and inoculated with AMF *Rhizophagus iregularis* to form CMN (red). The blue double-head arrow indicates the position of CMN interruption prior to sender plant wounding and *flg22* application to measure responses in the receiver plant leaves. **(B)** Volcano plots displaying down-regulated or up-regulated leaf metabolites (L) and volatile compounds (V) when comparing inter-plant responses to wound and *flg22* with H_2O controls in receivers with intact (top) or cut (bottom) CMN. **(C)** Hierarchical clustering of colour-coded log2 fold changes (FC) for all 53 detected leaf metabolites and all 27 detected volatiles. Two clusters of compounds display the largest relative differences in receiver responses to inter-plant stress signals between connected (con) and cut CMN treatments. The asterisks indicate significant FC based on the volcano plots in panel **B**. Chemical structures are based on ChemSpider and PubChem databases for the closest matching compounds. **(D)** The network produced by regularized canonical correspondence analysis displays the correlation between normalized CPMS read counts of 4885 DEGs (identified in Fig. 1) with relative metabolite quantities of the same plant. Only correlations with threshold >0.7 are displayed and include 4 metabolites (orange). The available homology-based gene function predictions from MtrunR108_HiC reference genome are mapped on the network along with the gene expression changes in CMN connected receivers as depicted in panel **A**. The source data for network generation, gene IDs, gene and metabolite descriptions for Figure 3 are provided in the **Supplemental Table 4.**

Interestingly, proline and its derivatives pyrroline-5-carboxylate are involved in plant responses to abiotic and biotic stress, including pathogens defence and mitigation of oxidative damage by scavenging reactive oxygen species (ROS) (Qamar *et al.*, 2015; Siddique *et al.*, 2018). Moreover, soyasapogenols are important legume triterpenoids that act as phytoanticipins (preformed defense compounds) and phytoalexins (induced defense compounds), contributing to defences against pathogens by perturbing microbial membrane integrity (Szakiel *et al.*, 2011; Suzuki *et al.*, 2019). The highly correlated MYB, GRAS and other transcription factor families may indicate their regulatory pathways while the correlated expression of cell wall proteins and transmembrane proteins (**Figure 3D)** may be linked to the saponin mechanisms of action.

Ethyl-d-glucosides have been found in tomato root exudates and function as chemoattractant of phytopathogenic bacterium *Ralstonia solanacearum* (Hasegawa *et al.*, 2018). Other glucopyranosides are reported to be induced upon herbivory (Günther *et al.*, 2019). α-muurolene along with other terpenoids from endophytes of *Catharanthus roseus* displayed antifungal properties (Yan *et al.*, 2018).

CMN mediated inter-plant signals induce acquired susceptibility to Botrytis cinerea but resistance to Fusarium sporotrichoides

Next, we wished to test whether stressed sender plants modulate resistance to pathogens in CMN connected receivers. When we added generalist fungal pathogen *Botrytis cinerea* to naïve receiver plants, the necrotic lesions were significantly larger when sender plants were wounded and treated with flagellin compared to water treated senders (**Figure 4**), suggesting inter-plant signal induced susceptibility to the pathogen attack. Surprisingly, this effect was the opposite to intra-plant signals induced by wounding and flagellin which reduced lesion size in *B. cinerea* infected distal leaves (**Supplemental Figure 2**). Furthermore, when we exposed naïve receiver plants to another fungal pathogen *Fusarium sporotrichoides*, the necrotic lesions were significantly smaller when CMN-connected sender plants were wounded and treated with flagellin compared to water treated senders (**Figure 4**). This strongly indicates that stress induced inter-plant signals in mycorrhiza connected plants have species specific effects on receiver tolerance to different fungal pathogens.

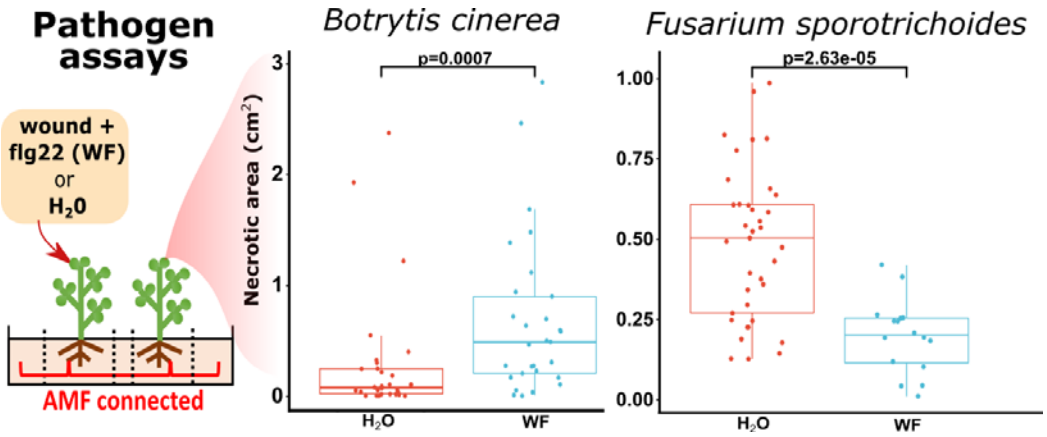

Figure 4. Stress-induced inter-plant signals modulate resistance to fungal pathogens in CMN connected plants. Size of necrotic lesions on *Mediago truncatula* leaves 72 after inoculation with *Botrytis cinerea* and *Fusarium sporotichoides*. Wounding and flagellin treatment of sender plants induces resistance to *F. sporotrichoides* (two-tailed t-test=4.621; p= 2.629e-05) but susceptibility to *B. cinerea* (Mann Whitney U=220; p=0.000697). Pathogen assays were repeated independently 3-times and represented as pooled data. Line indicates the median, boxes represent the interquartile range (IQR), whiskers - variance within 1.5xIQR.

Discussion

CMN act as underground internet for plant information exchange

Several studies have highlighted the role of stem-parasitic dodder (*Cuscuta sp.*) in transferring herbivory (Hettenhausen *et al.*, 2017) as well as salt and nutrient stress (Li *et al.*, 2020) signals from plant to plant. In these examples, the parasitic plant effectively acts as biological ''bridge'' in the exchange of mobile molecular signals and establishing ''wired'' inter-plant connections (Sharifi & Ryu, 2020). Analogous to wired ethernet connections in IT, CMN has been hypothesised to function as plant ''underground internet'' or ''information exchange superhighway'' (Bais *et al.*, 2004; Barto *et al.*, 2012; Khashi u Rahman *et al.*, 2019). However, to date our mechanistic understanding on the molecular responses to stress in mycorrhizae-interconnected plants have been limited. Here we identified markedly different volatile, leaf metabolite and transcriptional profile of *Medicago* plants that share intact AMF-connection with biotic stress stimulated signal senders compared to plants with interrupted AMF-connection (**Fig. 1, Fig. 3**). Furthermore, this manifested in altered plant susceptibility to pathogenic fungi *Botrytis cinerea* and *Fusarium sporotrichoides* **(Fig.4)**. Together our study provides strong support to the hypothesis that mycorrhizae likely act as an important network for information exchange within plant communities in nature.

This compliments findings by other groups where CMN has been shown to mediate dynamic redistribution of carbon resources between aphid attacked wheat or nematode infested potato (Charters *et al.*, 2020; Bell *et al.*, 2022) and their naïve conspecific neighbours. Similarly, CMN participates in carbon redistribution between orchid hosts of different developmental stages (Read *et al.*, 2024). Together with our findings, this underscores that CMNs likely act as mediators and regulators of inter-plant nutrient and signal exchange in diverse monocot and eudicot species. However,

it remains to be studied whether such CMN effects are host species-dependent and act in transferring biologically relevant signals between different host species. Given that CMN mediates carbon flow between hosts in response to biotic stress (Charters *et al.*, 2020; Bell *et al.*, 2022), it is possible that herbivory or pathogen induced molecular signals may follow the dynamics of bulk water flow and carbon sink-source relationships, which should be tested in future experiments. Likewise, the properties and composition of the inter-plant signal itself remains yet elusive. Based on the extensive research about within-plant systemic signals (Steinhorst & Kudla, 2013; Farmer *et al.*, 2020; Gao *et al.*, 2021) potential candidates for mycelial transmitted plant-to-plant signals could involve electrical signals, Ca^{2+} waves, small metabolites as well as biotic stress and symbiosis induced small mobile RNA species (Šečić *et al.*, 2021a; Schäfer, 2021) transported via plant (Borniego & Innes, 2023) or fungal (Rutter & Innes, 2023) extracellular vesicles (EVs). EVs have been implicated in different plant-pathogen, plant-endophyte and mycorrhizal interactions (Lefebvre & Lécuyer, 2017; Hua *et al.*, 2018; Cai *et al.*, 2018; Mewalal *et al.*, 2019; Šečić & Kogel, 2021; Šečić *et al.*, 2021b)

Ecological and evolutionary relevance of CMN-mediated inter-plant signals

CMN transmitted plant stress signals were shown to benefit the receiver by providing increased pathogen resistance (Song *et al.*, 2010) and recruitment of natural enemies (Babikova *et al.*, 2013). This prompted an unchallenged belief that CMN are strictly beneficial based on the systems studied thus far. However, our data on differential inter-plant *M. truncatula* responses to *B. cinerea* and *F. sporotrichoides* infection suggest that the potential beneficial effects from eavesdropping on conspecific signals via CMN must be holistically studied in context of different pest and pathogen species as well as host genotypes. Intriguingly, neighbour-modulated susceptibility (NMS) has been documented in rice and durum wheat growing next to pathogen free conspecifics of different genotypes and appears to be mediated by inter-plant signals in soil (Pélissier *et al.*, 2021). In particular, the study showed that wheat growing next to a different conspecific genotype display increased susceptibility to hemibiotroph *Zimenoseptoria tritici* but reduced susceptibility to biotroph *Puccinia triticina*, suggesting different production or perception of signals by different plant genotypes. Similarly, *Magnoporthe oryzae* showed fewer lesions on rice neighbouring a different conspecific genotype compared to isogenic cultivar, while another hemibiotroph *Bipolaris oryzae* demonstrated more lesions (Pélissier *et al.*, 2021). *Arabidopsis* plants exposed to elicitors in insect eggs are able to produce inter-plant signals that induce broad spectrum resistance against bacterial pathogen *Pseudomonas syringae* (Orlovskis & Reymond, 2020) and fungus *Botrytis cinerea* (Alfonso *et al.*, 2021), suggesting that certain plant-to-plant signals may be potentially more conserved and less specific. This further highlights the need to test a range of different elicitors on senders and evaluate responses in responders of different genotypes and species in the future experiments.

Neighbour induced susceptibility or resistance would provide opposing selective pressures for the evolution of specific signal generation and perception mechanisms along with receiver responses. Kalske *et al.* (2019) demonstrated kin selection on herbivory-driven inter-plant VOC signals that benefit receivers by

increasing resistance to pest attack. CMNs incorporate additional layer of complexity by considering benefits (or neutral effects) to mycorrhizal fungi from modulating biotic stress responses in receivers.

Within natural environments plant wired and wireless signals may frequently coincide, therefore it is necessary to consider multiple parallel signals and experimentally manipulate or eliminate one at a time. The experimental design herein allowed volatile, root exudate and CMN-mediated inter-plants signal exchange between neighbours. By cutting the CMN, we have highlighted the contribution of CMN in the background of other "wired" and "wireless" inter-plant signals and illuminated those receiver plant responses that depend on the presence of intact CMN versus interrupted network. Crucially, **Supplemental Fig. 3** suggests that physical tampering of AMF hyphae and soil outside the established plant-to-plant CMN connection *per-se* does not significantly alter plant responses. Instead, the interruption of CMN dramatically alters plant transcriptional as well as metabolic responses (**Fig. 1-3**) which may be triggered by a combination of sender volatiles, exudates and CMN mediated signals.

CMN contribution to inter-plant modulation of plant defence and metabolism

Mevalonate is one of the precursors for isoprenoid biosynthesis, including monoterpenes, sesquiterpenes and triterpenes via the activity of many CYP450s and UDP-glycosyltransferases (UGTs) (Fukushima *et al.*, 2013). Intact CMN was important for inter-plant signal receivers to display increased triterpenoid saponin production (including bayogenin (L42), medicagenic acids and their derivatives L45-L47) in response to sender wounding and *flg22* treatment (**Fig. 3B**). Additionally, levels of numerous monoterpene leaf volatiles were among the most notable differences between receivers in intact CMN and cut CMN pots (**Fig. 3C**), suggesting that mycorrhizal mediated signals from elicited sender plants contribute to changes in both volatile and leaf metabolite content and could explain different defensive phenotypes against *Botrytis* and *Fusarium*. For example, medicagenic acids, bayogenin and other saponins are important specialized metabolites involved in herbivore and pathogen defence (Szakiel *et al.*, 2011; Da Silva *et al.*, 2012; D'Addabbo *et al.*, 2020; Norvienyeku *et al.*, 2021). Similarly, many of the volatile monoterpenoids differentially regulated in the cut and intact CMN pots play important roles in pollinator attractions and defence against herbivores and pathogens. Since *Medicago truncatula* is primarily a self-pollinator, it is unlikely that the altered VOC profiles would affect plant reproductive fitness directly. However, volatile monoterpenes have been shown to induce inter-plant systemic acquired resistance (SAR) (Riedlmeier *et al.*, 2017) and could relay the signals from plant-to-plant (Wenig *et al.*, 2019). Intriguingly, whether VOCs could further propagate and amplify CMN-mediated inter-plant signals within community remains to be tested in the future.

Our study described the pre-activation of plant defences in receivers prior to a potential pathogen attack. For example, ethyl-d-gluccopiranoside (L9) and genistein 7-O-glucoside (L15) may be phytoanticipins - glycosylated forms of potentially toxic compounds after cleavage of the sugar molecule upon following pathogen attack. Another metabolite significantly increased in receivers with intact CMN is 1H-Indole-

3-acetaldehyde (IAAld) (L3) – an intermediate for auxin synthesis. As reviewed by Spaepen *et al.* (2007) auxins have important roles in plant-microbe interactions. Curiously, *P. syringae* strain DC3000 produces IAA as a plant virulence factor from IAAld using dehydrogenase AldA in order to supress salicylic acid-mediated defenses in *A. thaliana* (McClerklin *et al.*, 2018). We hypothesise that metabolites like IAAld could potentially also function as *Medicago* defence priming factors. Therefore, future experiments should compare inter-plant responses after the pathogen attack to better characterise such priming effects – responses that remain conditioned but ''silent'' in absence of the attack. Comparison of receiver responses before (this study) and after pathogen attach may better describe the susceptibility factors and resistance factors that are important in pathogen species specific interactions.

We found that plant responses to CMN-mediated stress-induced sender signals are highly enriched in gene functions related to defence responses and signalling **(Fig. 2)**. Additionally, we found that certain metabolite production is highly correlated with defence gene expression and gene functions related to transcription factors (TFs) and hormone responses (**Fig. 3C**). For example, expression of several GRAS family *SCARECROW (SCR)* TFs and DELLA-related gibberellin response factors are negatively correlated with sapogenin and proline production but positively correlated with vacuolar auxin transporter WALLS ARE THIN1 (WAT1) which is also involved in cell wall thickening (Ranocha *et al.*, 2013). Given that many cell wall biosynthesis genes were downregulated (**Fig. 2**) and IAAld production is increased in receivers (**Fig. 3B**) with the intact CMN network, we hypothesise that auxin homeostasis may in part contribute to cell wall remodelling and specialized metabolite production in defence against pathogens. Moreover, gene and metabolite correlation analysis highlights (**Fig. 3D**) multiple possible links between other plant transport protein functions such as sucrose or metal transporters, NIP family aquaporins, known for involvement in AMF symbiosis and plant-pathogen interactions (Afzal *et al.*, 2016), and specialized metabolites. Such links will be tested in future experiments and may yield novel discoveries of plant defence regulation during symbiosis and interactions with signals from neighbours.

Data availability

RNA-seq raw data (fastq) are uploaded to NCBI under BioProject: **PRJNA1186668**.

Author contributions (Contributor Role Taxonomy CRediT):

ZO: conceptualization and experimental design (1), data curation (2), formal analysis (3), funding acquisition (4), investigation (5), methodology (6), project administration (7), reagent acquisition and lab resource planning (8), student supervision (10), data validation (11), statistical analysis and visualisation (12), writing (13), reviewing and editing the original manuscript (14)

EV: formal analysis (3) of pathogen data, investigation – plant-pathogen assays (5), reviewing and editing the original manuscript (14)

DP: investigation – experiment setup, RNA extractions, rt-qPCR (5), reviewing and editing the original manuscript (14)

AK: investigation – experiment setup, RNA extractions, rt-qPCR (5), reviewing and editing the original manuscript (14)
KTB: investigation – experiment setup, RNA extractions, rt-qPCR (5), reviewing and editing the original manuscript (14)
IN: investigation – metabolic analysis (5), reviewing and editing the original manuscript (14)
IS: data curation (2), formal analysis (3) of RNA-seq data, reviewing and editing the original manuscript (14)
SJL: conceptualization and experimental design (1), methodology (6), reviewing and editing the original manuscript (14)

Funding
This work was supported by Latvian Council of Science Fundamental and Applied Research grant lzp-2021/1-0056 awarded to ZO and University of Latvia Fundation (*SIA MikroTik* donation).

Acknowledgements
We are grateful to Prof. Yves Poirier group (DBMV, University of Lausanne) for the generous donation of *Medicago truncatula* R108 seeds. We also thank BMC Genome Centre and Bioinformatics Unit support staff for assistance during sequencing and raw data handling.

Competing interest
The authors declare no competing interests.

Literature Cited

Afzal Z, Howton TC, Sun Y, Mukhtar MS. **2016**. The Roles of Aquaporins in Plant Stress Responses. *Journal of Developmental Biology* **4**: 9.

Alfonso E, Stahl E, Glauser G, Bellani E, Raaymakers TM, Van den Ackerveken G, Zeier J, Reymond P. **2021**. Insect eggs trigger systemic acquired resistance against a fungal and an oomycete pathogen. *New Phytologist* **232**: 2491–2505.

Antonopoulou I, Sapountzaki E, Rova U, Christakopoulos P. **2022**. Ferulic Acid From Plant Biomass: A Phytochemical With Promising Antiviral Properties. *Frontiers in Nutrition* **8**.

Babikova Z, Gilbert L, Bruce TJA, Birkett M, Caulfield JC, Woodcock C, Pickett JA, Johnson D. **2013**. Underground signals carried through common mycelial networks warn neighbouring plants of aphid attack. *Ecology Letters* **16**: 835–843.

Bahadur A, Batool A, Nasir F, Jiang S, Mingsen Q, Zhang Q, Pan J, Liu Y, Feng H. **2019**. Mechanistic Insights into Arbuscular Mycorrhizal Fungi-Mediated Drought Stress Tolerance in Plants. *International Journal of Molecular Sciences* **20**: 4199.

Bai L, Wang W, Hua J, Guo Z, Luo S. **2020**. Defensive functions of volatile organic compounds and essential oils from northern white-cedar in China. *BMC Plant Biology* **20**: 1–9.

Bais HP, Park S-W, Weir TL, Callaway RM, Vivanco JM. **2004**. How plants communicate using the underground information superhighway. *Trends in Plant Science* **9**: 26–32.

Baranski R. **2008**. Genetic Transformation of Carrot (Daucus carota) and Other Apiaceae Species. *Transgenic Plant Journal* **2**: 18–38.

Barto EK, Weidenhamer JD, Cipollini D, Rillig MC. **2012**. Fungal superhighways: do common mycorrhizal networks enhance below ground communication? *Trends in Plant Science* **17**: 633–637.

Bell CA, Magkourilou E, Urwin PE, Field KJ. **2022**. Disruption of carbon for nutrient exchange between potato and arbuscular mycorrhizal fungi enhanced cyst nematode fitness and host pest tolerance. *New Phytologist* **234**: 269–279.

Boncan DAT, Tsang SSK, Li C, Lee IHT, Lam H-M, Chan T-F, Hui JHL. **2020**. Terpenes and Terpenoids in Plants: Interactions with Environment and Insects. *International Journal of Molecular Sciences* **21**: 7382.

Borniego ML, Innes RW. **2023**. Extracellular RNA: mechanisms of secretion and potential functions (P Manavella, Ed.). *Journal of Experimental Botany* **74**: 2389–2404.

Brambilla A, Sommer A, Ghirardo A, Wenig M, Knappe C, Weber B, Amesmaier M, Lenk M, Schnitzler J-P, Vlot AC. **2022**. Immunity-associated volatile emissions of β-ionone and nonanal propagate defence responses in neighbouring barley plants. *Journal of Experimental Botany* **73**: 615–630.

Brundrett MC, Tedersoo L. **2018**. Evolutionary history of mycorrhizal symbioses and global host plant diversity. *New Phytologist* **220**: 1108–1115.

Cai Q, Qiao L, Wang M, He B, Lin F-M, Palmquist J, Huang S-D, Jin H. **2018**. Plants send small RNAs in extracellular vesicles to fungal pathogen to silence virulence genes. *Science* **360**: 1126–1129.

Charters MD, Sait SM, Field KJ. **2020**. Aphid Herbivory Drives Asymmetry in Carbon for Nutrient Exchange between Plants and an Arbuscular Mycorrhizal Fungus. *Current Biology* **30**: 1801-1808.e5.

Da Silva P, Eyraud V, Carre-Pierrat M, Sivignon C, Rahioui I, Royer C, Gressent F. **2012**. High toxicity and specificity of the saponin 3-GlcA-28-AraRhaxyl-medicagenate, from Medicago truncatula seeds, for Sitophilus oryzae. *BMC Chemical Biology* **12**: 1–9.

D'Addabbo T, Argentieri MP, Żuchowski J, Biazzi E, Tava A, Oleszek W, Avato P. **2020**. Activity of Saponins from Medicago Species against Phytoparasitic Nematodes. *Plants* **9**: 443.

Dobin A, Gingeras TR. **2015**. Mapping RNA-seq Reads with STAR. *Current protocols in bioinformatics / editoral board, Andreas D. Baxevanis ... [et al.]* **51**: 11.14.1-11.14.19.

Dong Y, Wei Z, Zhang W, Li J, Han M, Bai H, Li H, Shi L. **2024**. LaMYC7, a positive regulator of linalool and caryophyllene biosynthesis, confers plant resistance to Pseudomonas syringae. *Horticulture Research* **11**: uhae044.

Farmer EE, Gao Y-Q, Lenzoni G, Wolfender J-L, Wu Q. **2020**. Wound- and mechanostimulated electrical signals control hormone responses. *New Phytologist* **227**: 1037–1050.

Francis R, Read DJ. **1984**. Direct transfer of carbon between plants connected by vesicular–arbuscular mycorrhizal mycelium. *Nature* **307**: 53–56.

Fukushima EO, Seki H, Sawai S, Suzuki M, Ohyama K, Saito K, Muranaka T. **2013**. Combinatorial Biosynthesis of Legume Natural and Rare Triterpenoids in Engineered Yeast. *Plant and Cell Physiology* **54**: 740–749.

Gao H, Guo M, Song J, Ma Y, Xu Z. **2021**. Signals in systemic acquired resistance of plants against microbial pathogens. *Molecular Biology Reports* **48**: 3747–3759.

Gesell A, Blaukopf M, Madilao L, Yuen MMS, Withers SG, Mattsson J, Russell JH, Bohlmann J. **2015**. The Gymnosperm Cytochrome P450 CYP750B1 Catalyzes Stereospecific Monoterpene Hydroxylation of (+)-Sabinene in Thujone Biosynthesis in Western Redcedar. *Plant Physiology* **168**: 94–106.

Günther J, Lackus ND, Schmidt A, Huber M, Stödtler H-J, Reichelt M, Gershenzon J, Köllner TG. **2019**. Separate Pathways Contribute to the Herbivore-Induced Formation of 2-Phenylethanol in Poplar. *Plant Physiology* **180**: 767–782.

Hasegawa T, Okabe A, Kato Y, Ooshiro A, Kawaide H, Natsume M. **2018**. Ethyl β-d-glucoside: a novel chemoattractant of Ralstonia solanacearum isolated from tomato root exudates by a bioassay-guided fractionation. *Bioscience, Biotechnology, and Biochemistry* **82**: 2049–2052.

Hettenhausen C, Li J, Zhuang H, Sun H, Xu Y, Qi J, Zhang J, Lei Y, Qin Y, Sun G, *et al.* 2017. Stem parasitic plant Cuscuta australis (dodder) transfers herbivory-induced signals among plants. *Proceedings of the National Academy of Sciences* **114**: E6703–E6709.

Hua C, Zhao J-H, Guo H-S. **2018**. Trans-Kingdom RNA Silencing in Plant–Fungal Pathogen Interactions. *Molecular Plant* **11**: 235–244.

Jiao C, Gong J, Guo Z, Li S, Zuo Y, Shen Y. **2022**. Linalool Activates Oxidative and Calcium Burst and CAM3-ACA8 Participates in Calcium Recovery in Arabidopsis Leaves. *International Journal of Molecular Sciences* **23**: 5357.

Kalske A, Shiojiri K, Uesugi A, Sakata Y, Morrell K, Kessler A. **2019**. Insect Herbivory Selects for Volatile-Mediated Plant-Plant Communication. *Current Biology* **29**: 3128-3133.e3.

Khashi u Rahman M, Zhou X, Wu F. **2019**. The role of root exudates, CMNs, and VOCs in plant–plant interaction. *Journal of Plant Interactions* **14**: 630–636.

Kopylova E, Noé L, Touzet H. **2012**. SortMeRNA: fast and accurate filtering of ribosomal RNAs in metatranscriptomic data. *Bioinformatics* **28**: 3211–3217.

Kumar A, Verma JP. **2018**. Does plant-Microbe interaction confer stress tolerance in plants: A review? *Microbiological Research* **207**: 41–52.

Lefebvre FA, Lécuyer E. **2017**. Small Luggage for a Long Journey: Transfer of Vesicle-Enclosed Small RNA in Interspecies Communication. *Frontiers in Microbiology* **8**.

Li S, Zhang J, Liu H, Liu N, Shen G, Zhuang H, Wu J. **2020**. Dodder-transmitted mobile signals prime host plants for enhanced salt tolerance (R Hancock, Ed.). *Journal of Experimental Botany* **71**: 1171–1184.

Liu S, Jiang J, Ma Z, Xiao M, Yang L, Tian B, Yu Y, Bi C, Fang A, Yang Y. **2022**. The Role of Hydroxycinnamic Acid Amide Pathway in Plant Immunity. *Frontiers in Plant Science* **13**.

Lohse M, Nagel A, Herter T, May P, Schroda M, Zrenner R, Tohge T, Fernie AR, Stitt M, Usadel B. **2014**. Mercator: a fast and simple web server for genome scale functional annotation of plant sequence data: Mercator: sequence functional annotation server. *Plant, Cell & Environment* **37**: 1250–1258.

McClerklin SA, Lee SG, Harper CP, Nwumeh R, Jez JM, Kunkel BN. **2018**. Indole-3-acetaldehyde dehydrogenase-dependent auxin synthesis contributes to virulence of Pseudomonas syringae strain DC3000. *PLOS Pathogens* **14**: e1006811.

Mewalal R, Yin H, Hu R, Jawdy S, Vion P, Tuskan GA, Le Tacon F, Labbé JL, Yang X. **2019**. Identification of Populus Small RNAs Responsive to Mutualistic Interactions With Mycorrhizal Fungi, Laccaria bicolor and Rhizophagus irregularis. *Frontiers in Microbiology* **10**: 515.

Murata M, Kobayashi T, Seo S. **2020**. α-Ionone, an Apocarotenoid, Induces Plant Resistance to Western Flower Thrips, Frankliniella occidentalis, Independently of Jasmonic Acid. *Molecules* **25**: 17.

Norvienyeku J, Lin L, Waheed A, Chen X, Bao J, Aliyu SR, Lin L, Shabbir A, Batool W, Zhong Z, *et al.* 2021. Bayogenin 3-O-cellobioside confers non-cultivar-specific defence against the rice blast fungus Pyricularia oryzae. *Plant Biotechnology Journal* **19**: 589–601.

Orlovskis Z, Reymond P. **2020**. Pieris brassicae eggs trigger interplant systemic acquired resistance against a foliar pathogen in Arabidopsis. *New Phytologist* **228**: 1652–1661.

Orlovskis Z, Singh A, Kliot A, Huang W, Hogenhout SA. **2024**. Phytoplasma Targeting of MADS-Box Factor SVP Suppresses Leaf Responses to Insect Vector Males, Promoting Female Attraction and Colonization. *eLife* **13**.

Pélissier R, Buendia L, Brousse A, Temple C, Ballini E, Fort F, Violle C, Morel J-B. **2021**. Plant neighbour-modulated susceptibility to pathogens in intraspecific mixtures. *Journal of Experimental Botany* **72**: 6570–6580.

Pieterse CMJ, Leon-Reyes A, Van der Ent S, Van Wees SCM. **2009**. Networking by small-molecule hormones in plant immunity. *Nature Chemical Biology* **5**: 308–316.

Qamar A, Mysore K, Senthil-Kumar M. **2015**. Role of proline and pyrroline-5-carboxylate metabolism in plant defense against invading pathogens. *Frontiers in Plant Science* **6**.

Raguso RA, Pichersky E. **1999**. New Perspectives in Pollination Biology: Floral Fragrances. A day in the life of a linalool molecule: Chemical communication in a plant□pollinator system. Part 1: Linalool biosynthesis in flowering plants. *Plant Species Biology* **14**: 95–120.

Ranocha P, Dima O, Nagy R, Felten J, Corratgé-Faillie C, Novák O, Morreel K, Lacombe B, Martinez Y, Pfrunder S, *et al.* 2013. Arabidopsis WAT1 is a vacuolar auxin transport facilitator required for auxin homoeostasis. *Nature Communications* **4**: 2625.

Read DJ, Haggar J, Magkourilou E, Durant E, Johnson D, Leake JR, Field KJ. **2024**. Photosynthate transfer from an autotrophic orchid to conspecific heterotrophic protocorms through a common mycorrhizal network. *New Phytologist* **243**: 398–406.

Riedlmeier M, Ghirardo A, Wenig M, Knappe C, Koch K, Georgii E, Dey S, Parker JE, Schnitzler J-P, Vlot AC. **2017**. Monoterpenes Support Systemic Acquired Resistance within and between Plants. *The Plant Cell* **29**: 1440–1459.

Ritchie ME, Phipson B, Wu D, Hu Y, Law CW, Shi W, Smyth GK. **2015**. limma powers differential expression analyses for RNA-sequencing and microarray studies. *Nucleic Acids Research* **43**: e47.

Ron M, Kajala K, Pauluzzi G, Wang D, Reynoso MA, Zumstein K, Garcha J, Winte S, Masson H, Inagaki S, *et al.* 2014. Hairy Root Transformation Using Agrobacterium rhizogenes as a Tool for Exploring Cell Type-Specific Gene Expression and Function Using Tomato as a Model. *Plant Physiology* **166**: 455–469.

Rutter BD, Innes RW. **2023**. Extracellular Vesicles in Phytopathogenic Fungi. *Extracellular Vesicles and Circulating Nucleic Acids* **4**: 72–88.

Schäfer P. **2021**. microRNAs – Game-changers in plant symbioses. *Journal of Plant Physiology* **263**: 153459.

Šečić E, Kogel K-H. **2021**. Requirements for fungal uptake of dsRNA and gene silencing in RNAi-based crop protection strategies. *Current Opinion in Biotechnology* **70**: 136–142.

Šečić E, Kogel K-H, Ladera-Carmona MJ. **2021a**. Biotic stress-associated microRNA families in plants. *Journal of Plant Physiology* **263**: 153451.

Šečić E, Zanini S, Wibberg D, Jelonek L, Busche T, Kalinowski J, Nasfi S, Thielmann J, Imani J, Steinbrenner J, *et al.* 2021b. A novel plant-fungal association reveals fundamental sRNA and gene expression reprogramming at the onset of symbiosis. *BMC Biology* **19**: 1–22.

Sharifi R, Ryu C-M. **2020**. Social networking in crop plants: Wired and wireless cross-plant communications. *Plant, Cell & Environment* **doi.org/10.1111/pce.13966**: 1–16.

Sharma E, Anand G, Kapoor R. **2017**. Terpenoids in plant and arbuscular mycorrhiza-reinforced defence against herbivorous insects. *Annals of Botany* **119**: 791–801.

Siddique A, Kandpal G, Kumar P. **2018**. Proline Accumulation and its Defensive Role Under Diverse Stress Condition in Plants: An Overview. *Journal of Pure and Applied Microbiology* **12**: 1655–1659.

Simard SW, Perry DA, Jones MD, Myrold DD, Durall DM, Molina R. **1997**. Net transfer of carbon between ectomycorrhizal tree species in the field. *Nature* **388**: 579–582.

Smith SE, Read DJ. **2008**. *Mycorrhizal Symbiosis.* Academic Press. 3rd ed.

Song Y, Chen D, Lu K, Sun Z, Zeng R. **2015**. Enhanced tomato disease resistance primed by arbuscular mycorrhizal fungus. *Frontiers in Plant Science* **6**: 786.

Song Y, Wang R, Wei X, Lu Y, Tang Z, Wu G, Su Y, Zeng R. **2011**. Mechanism of tomato plants enhanced disease resistance against early blight primed by arbuscular mycorrhizal fungus Glomus versiforme. *Ying Yong Sheng Tai Xue Bao = The Journal of Applied Ecology* **22**: 2316–2324.

Song YY, Ye M, Li CY, Wang RL, Wei XC, Luo SM, Zeng RS. **2013**. Priming of anti-herbivore defense in tomato by arbuscular mycorrhizal fungus and involvement of the jasmonate pathway. *Journal of Chemical Ecology* **39**: 1036–1044.

Song YY, Zeng RS, Xu JF, Li J, Shen X, Yihdego WG. **2010**. Interplant communication of tomato plants through underground common mycorrhizal networks. *PloS One* **5**: e13324.

Spaepen S, Vanderleyden J, Remans R. **2007**. Indole-3-acetic acid in microbial and microorganism-plant signaling. *FEMS Microbiology Reviews* **31**: 425–448.

St-Arnaud M, Hamel C, Vimard B, Caron M, Fortin JA. **1996**. Enhanced hyphal growth and spore production of the arbuscular mycorrhizal fungus Glomus intraradices in an in vitro system in the absence of host roots. *Mycological Research* **100**: 328–332.

Steinhorst L, Kudla J. **2013**. Calcium and Reactive Oxygen Species Rule the Waves of Signaling. *PLANT PHYSIOLOGY* **163**: 471–485.

Suzuki H, Fukushima EO, Shimizu Y, Seki H, Fujisawa Y, Ishimoto M, Osakabe K, Osakabe Y, Muranaka T. **2019**. Lotus japonicus Triterpenoid Profile and Characterization of the CYP716A51 and LjCYP93E1 Genes Involved in Their Biosynthesis In Planta. *Plant and Cell Physiology* **60**: 2496–2509.

Szakiel A, Pączkowski C, Henry M. **2011**. Influence of environmental biotic factors on the content of saponins in plants. *Phytochemistry Reviews* **10**: 493–502.

Tanruean K, Rakariyatham, Nuansri. **2014**. Efficient Synthesis of 4-Vinyl Guaiacol via Bioconversion of Ferulic Acid by Volvariella volvacea. *Chiang Mai J. Sci*.

Thimm O, Bläsing O, Gibon Y, Nagel A, Meyer S, Krüger P, Selbig J, Müller LA, Rhee SY, Stitt M. **2004**. mapman: a user-driven tool to display genomics data sets onto diagrams of metabolic pathways and other biological processes. *The Plant Journal* **37**: 914–939.

Tian T, Liu Y, Yan H, You Q, Yi X, Du Z, Xu W, Su Z. **2017**. agriGO v2.0: a GO analysis toolkit for the agricultural community, 2017 update. *Nucleic Acids Research* **45**: W122–W129.

Usadel B, Nagel A, Steinhauser D, Gibon Y, Bläsing OE, Redestig H, Sreenivasulu N, Krall L, Hannah MA, Poree F, *et al.* 2006. PageMan: an interactive ontology tool to generate, display, and annotate overview graphs for profiling experiments. *BMC bioinformatics* **7**: 535.

Usadel B, Nagel A, Thimm O, Redestig H, Blaesing OE, Palacios-Rojas N, Selbig J, Hannemann J, Piques MC, Steinhauser D, *et al.* 2005. Extension of the Visualization Tool MapMan to Allow Statistical Analysis of Arrays, Display of Coresponding Genes, and Comparison with Known Responses. *Plant Physiology* **138**: 1195–1204.

Vierheilig H, Coughlan AP, Wyss U, Piché Y. **1998**. Ink and Vinegar, a Simple Staining Technique for Arbuscular-Mycorrhizal Fungi. *Applied and Environmental Microbiology* **64**: 5004–5007.

Wenig M, Ghirardo A, Sales JH, Pabst ES, Breitenbach HH, Antritter F, Weber B, Lange B, Lenk M, Cameron RK, *et al.* 2019. Systemic acquired resistance networks amplify airborne defense cues. *Nature Communications* **10**: 3813.

Yan D-H, Song X, Li H, Luo T, Dou G, Strobel G. **2018**. Antifungal Activities of Volatile Secondary Metabolites of Four Diaporthe Strains Isolated from Catharanthus roseus. *Journal of Fungi* **4**: 65.

Yi Q, Park M-J, Vo KTX, Jeon J-S. **2024**. Polyamines in Plant–Pathogen Interactions: Roles in Defense Mechanisms and Pathogenicity with Applications in Fungicide Development. *International Journal of Molecular Sciences* **25**: 10927.

Zhou F, Emonet A, Dénervaud Tendon V, Marhavy P, Wu D, Lahaye T, Geldner N. **2020**. Co-incidence of Damage and Microbial Patterns Controls Localized Immune Responses in Roots. *Cell* **180**: 440-453.e18.

List of Supplemental tables

Supplemental Table 1: GO-term enrichment for the 1880 upregulated and 3005 downregulated receiver plant DEGs in the intact CMN treatment. Functional enrichment is based on Fisher exact test with Hochberg (FDR) correction using *agriGO v2.0*. Significantly enriched functions ($p<0.05$; $FDR<0.05$) for each ontology category – biological process, molecular function and cell compartment - are highlighted in bold and coloured.

Supplemental Table 2: *M. truncatula* R108 mapping file for MapMan functional bins generated by Mercator4 gene ortholog search and manual curation of plant defence and signalling category.

Supplemental Table 3: Intact CMN mediated functional gene responses of Medicago truncatula receiver plants to wound and flg22 treatment of sender plants.

Supplemental Table 4: Source data for rCCA and correlation network between transcriptome and metabolome datasets.

Supplemental data & figures

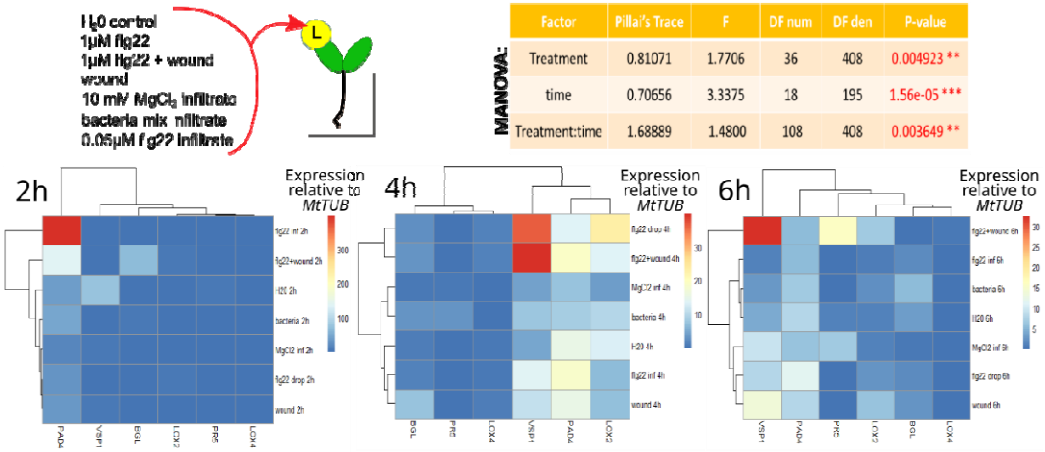

MANOVA:

Factor	Pillai's Trace	F	DF num	DF den	P-value
Treatment	0.81071	1.7706	36	408	0.004923 **
time	0.70656	3.3375	18	195	1.56e-05 ***
Treatment:time	1.68889	1.4800	108	408	0.003649 **

Supplemental Figure 1. Local expression of *Medicago trucnatula* immunity markers (*MtPAD4*, *MtVSP1*, *MtBGL*, *MtLOX2*, *MtLOX4*, *MtPR5*) relative to *MtTUB* reference gene 2h, 4h and 6h following the application of various stimuli on leaves: mechanical wounding by forceps (3x squeezing leaf blade), 5 µL drop of 1µM flg22, 5 µL drop of dH_2O (control), syringe infiltration of 0.05µM flg22, bacterial mix in 10mM $MgCl_2$ or sterile 10mM $MgCl_2$ as the control. Bacterial mix consisted of live suspension of overnight LB cultures of *Pseudomonas syringae*, *Dickeria chrysanthemi*, *Erwinia rhapontici*, *Pantotea agglomerans* at OD_{660}=0.0005 each. Heatmap displays average expression of 4 independent biological replicates. Each replicate was a pooled sample from two mature stimulated trifoliate leaves from separate plants. 2-factor Multiple Analysis of Variance (MANOVA) indicates significant changes in gene expression over the time-course and differences among the treatments.

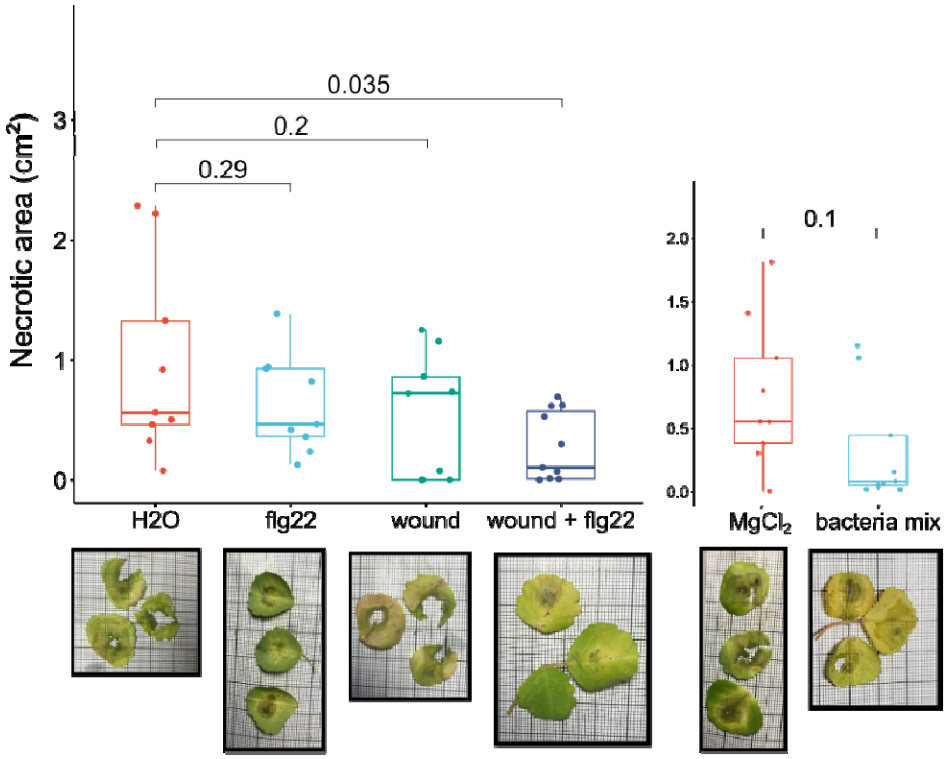

Supplemental Figure 2. Size of *Botrytis cinerea* necrotic lesions (72hpi) on systemic leaves after stimulation of distal leaves with the following treatments: 5µL drop of H_2O (control), 5 µL drop of 1µM flg22, wounding with forceps, wounding + 5 µL drop of 1µM flg22 as well as infiltrations10mM MgCl2 (control), live suspension of *P. syringae*, *D. chrysanthemi*, *E. rhapontici*, *P. agglomerans* at OD_{660}=0.0005 each in 10mM $MgCl_2$. All comparisons were performed at the same time. Box-plots depict distribution of individual data-points and means. ANOVA (F=2,86; p=0.18) suggest significant differences among the treatments and p-values from the Dunnet's two tailed t-test pairwise comparisons are depicted on top of the plots.

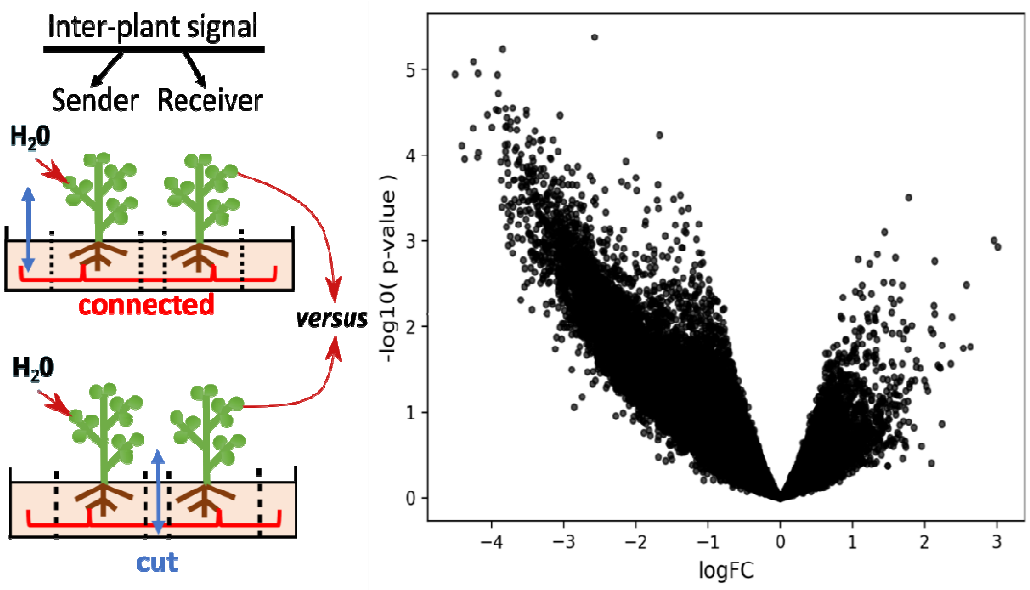

Supplemental Figure 3. No significantly differentially expressed genes (DEGs) were identified when comparing responder plants from intact-CNM and cut-CNM pots after sender plant treatment with water only. Volcano plot displays $\log_{10}$ of p-adj. and $\log_2$ of fold change for each transcript in the comparison.

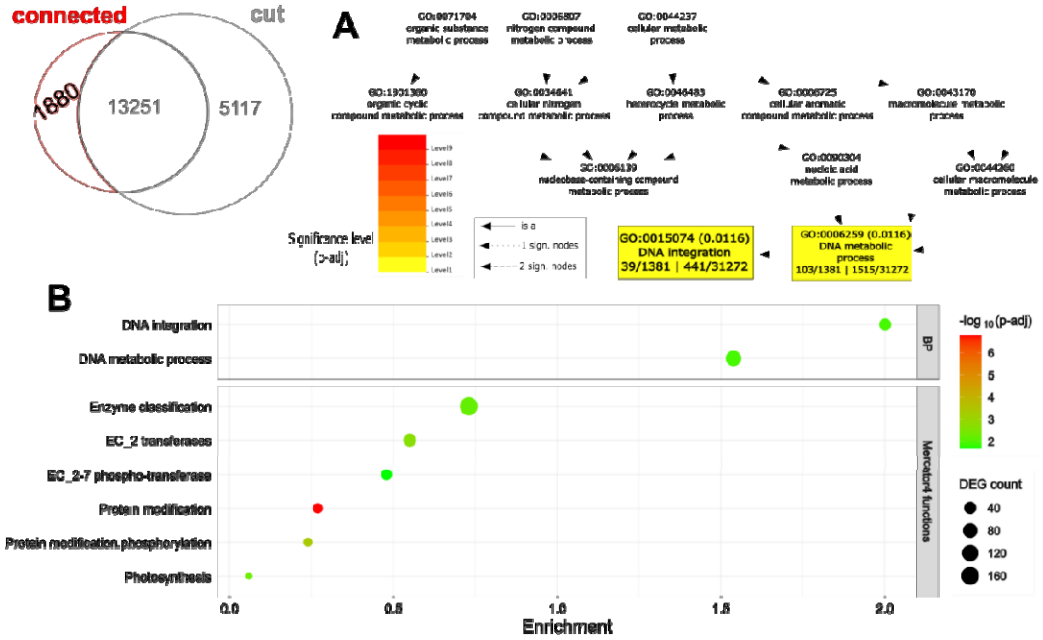

Supplemental Figure 4. Functional enrichment of GO-terms with 1880 upregulated responder plant DEGs in intact CMN pots. (**A**) GO-identifiers and their known or inferred hierarchical interactions. Boxes contain colour-coded FDR-corrected p-values, the number DEGs within the GO-term from the query list/total GO-annotations in the query list | total number genes corresponding to the GO-term/ total GO-annotations in the genome. (**B**) Bubble plots depicting the enrichment factor, number of DEGs and log10 normalized FDR-corrected (adj.) p-value for the enrichment significance. Only GO biological functions and Mercator4 functional predictions with p-adj.<0.05 are displayed. Full list of GO-terms and bins for functional enrichment analysis is available in **Supplemental Table 1.**

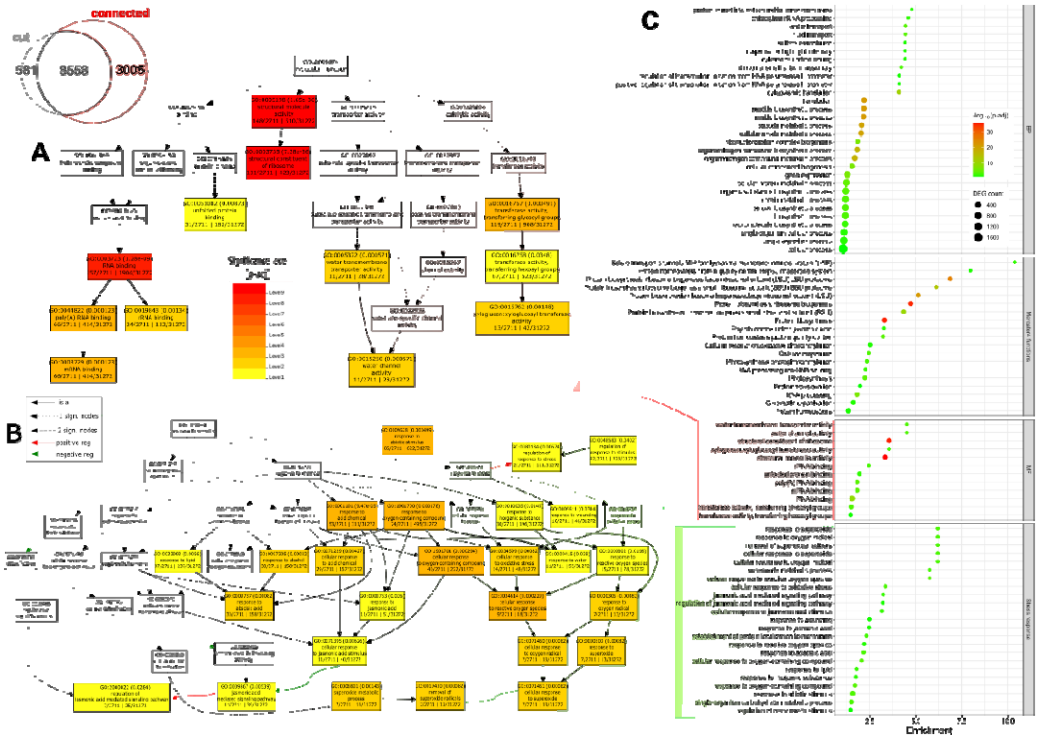

Supplemental Figure 5. Functional enrichment of GO-terms with 3005 downregulated responder plant DEGs in intact CMN pots. (**A**-**B**) GO-identifiers and their known or inferred hierarchical interactions. Boxes contain colour-coded FDR-corrected p-values, the number DEGs within the GO-term from the query list/total GO-annotations in the query list | total number genes corresponding to the GO-term/ total GO-annotations in the genome. Different arrow types indicate GO-terms associated to 1 or 2 other significant enriched functions as well as known positive or negative regulation between genes within the associated GO-term. (**A**) Enriched GO-identifiers for molecular functions (MF) related to RNA binding and ribosome functions. (**B**) Enriched GO-identifiers for biological processes related to ROS metabolism, response to stimuli and jasmonic acid, collectively displayed under Stress response cluster. (**C**) Bubble plots depicting the enrichment factor, number of DEGs and log10 normalized FDR-corrected (adj.) p-value for the enrichment significance. For brevity the plot displays the top 30 most sign. Enriched GO biological functions, all GO-terms for stress responses, all molecular functions and all Mercator4 functional predictions with p-adj.<0.05 are displayed. Full list of GO-terms and bins for functional enrichment analysis is available in **Supplemental Table 1.**

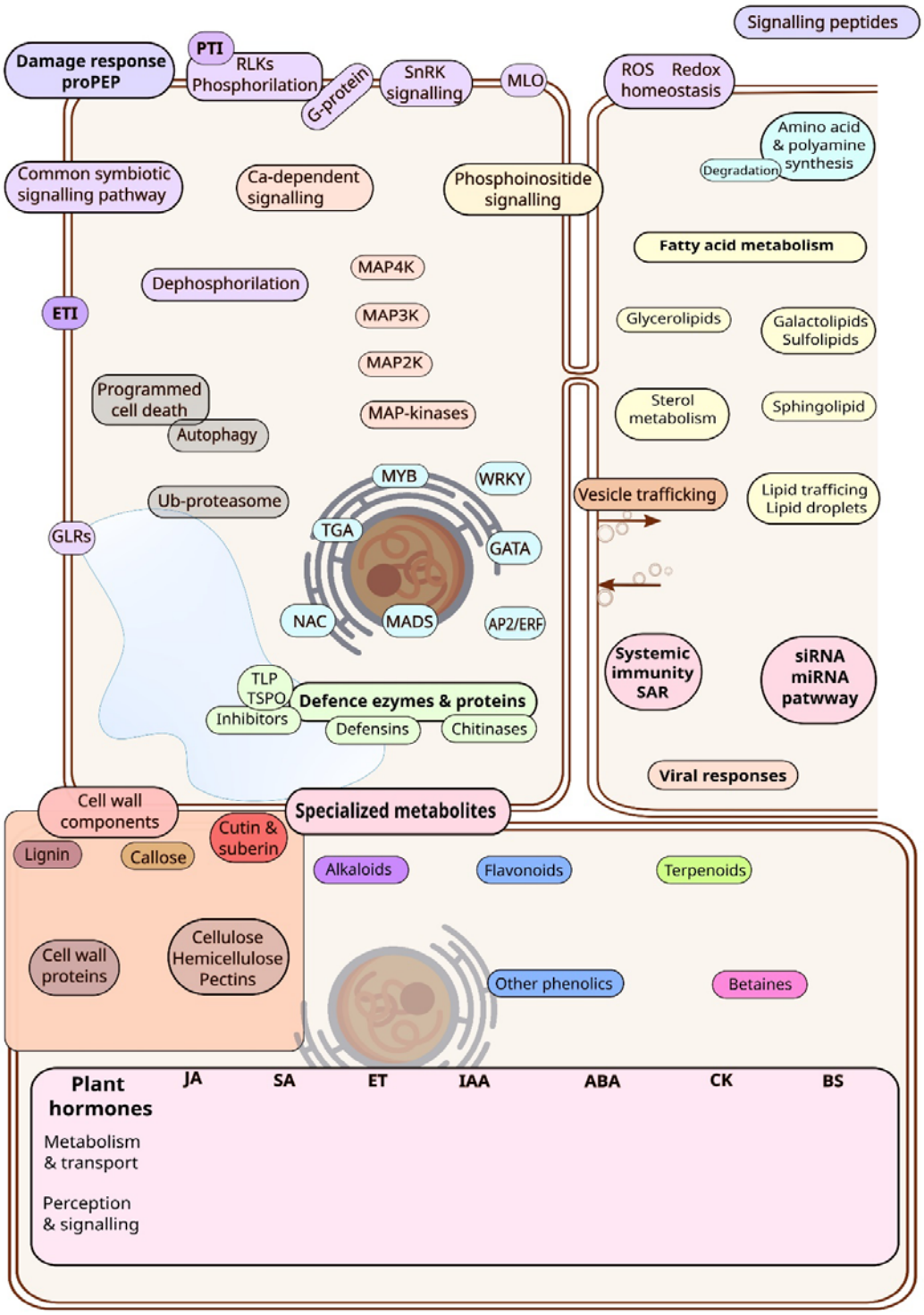

Supplemental figure 6. Image file for manually curated ‘’Defence signalling & response’’ category to display fold change of genes corresponding to bins listed in **Supplemental Table 2 tab-B.**

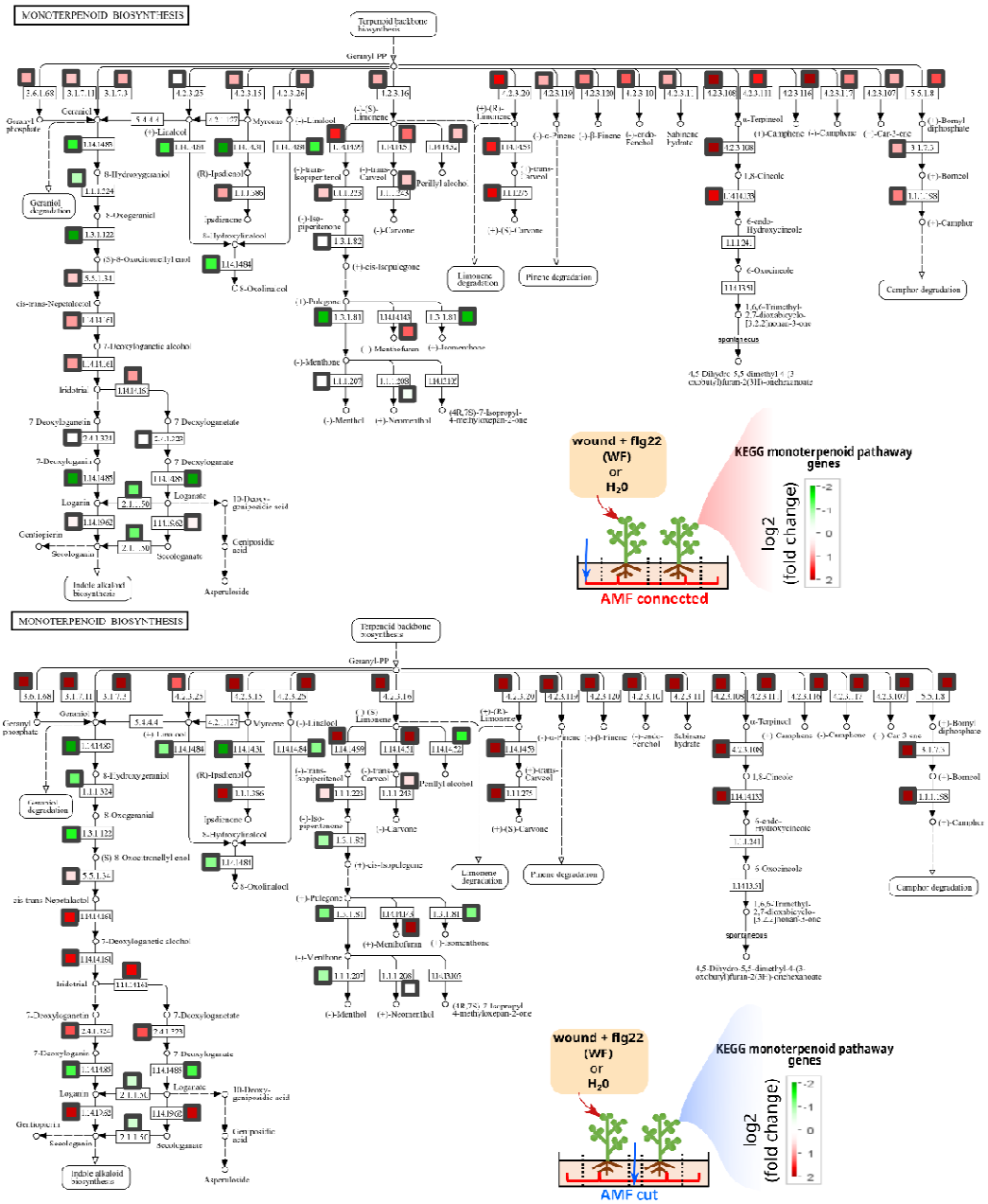

Supplemental figure 7. Monoterpene biosynthesis gene expression changes in responder plants to sender wounding and flg22 treatment compared to sender treatment with water. Top panel represents intact CMN, bottom panel – cut CMN. KEGG pathway map00902 was used to display RNA-seq data using the MapMan tool. The available protein sequences for each 00902 pathway gene were manually searched for the corresponding homologs in *M. trucatula R108* genome via MtrunR108_HiC portal blast tool.

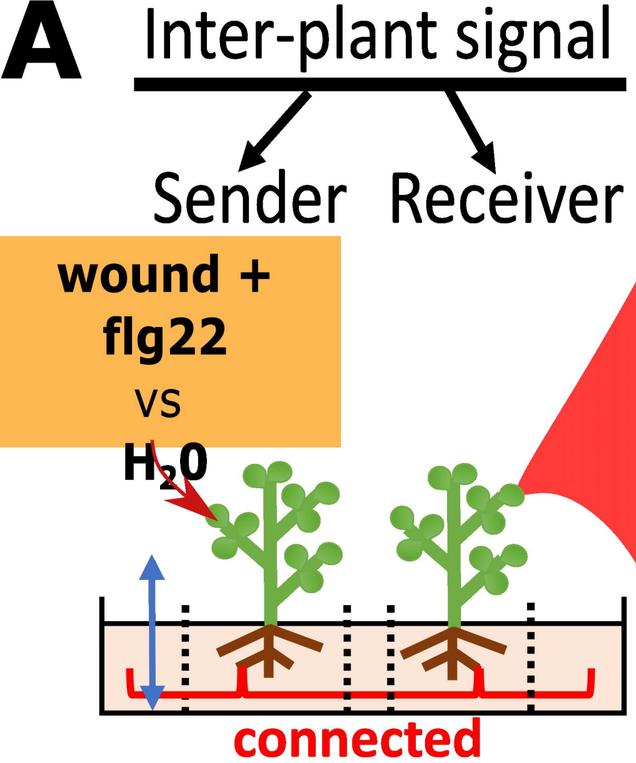
A
Inter-plant signal
Sender
Receiver
wound +
flg22
vs
H_2O
connected

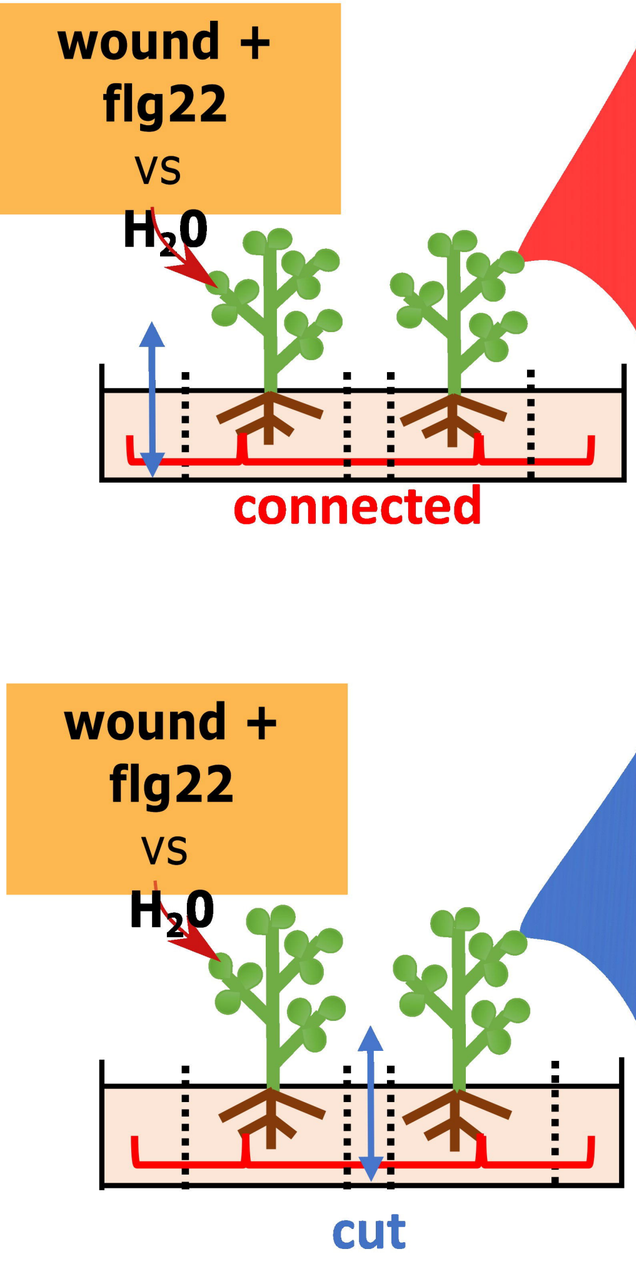
wound +
flg22
vs
H_2O
cut

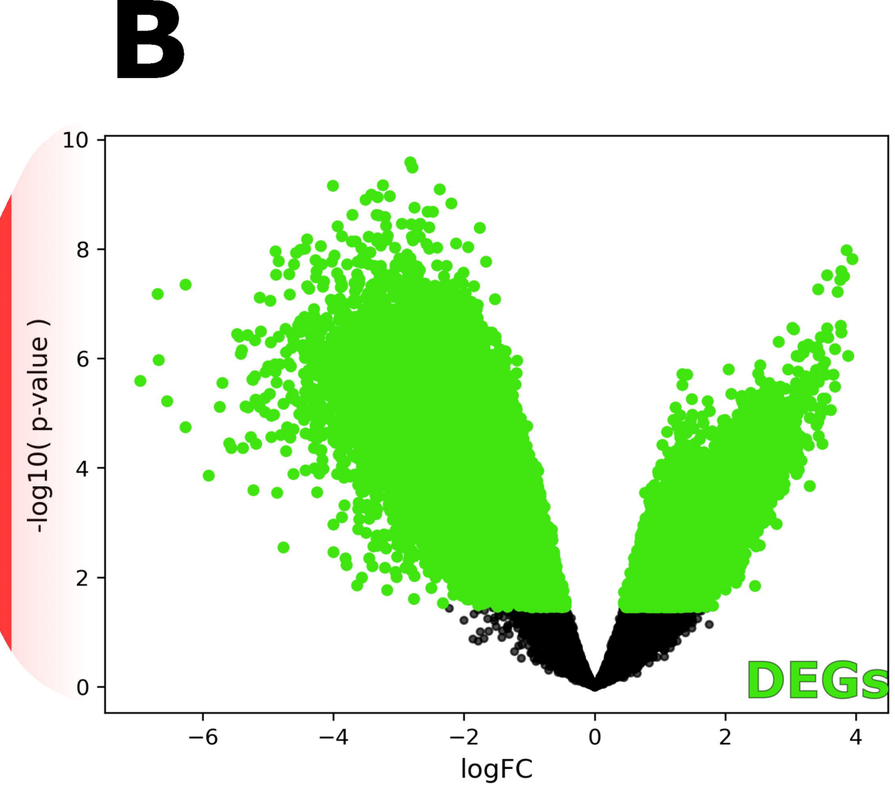
B
-log10(p-value)
logFC
DEGs

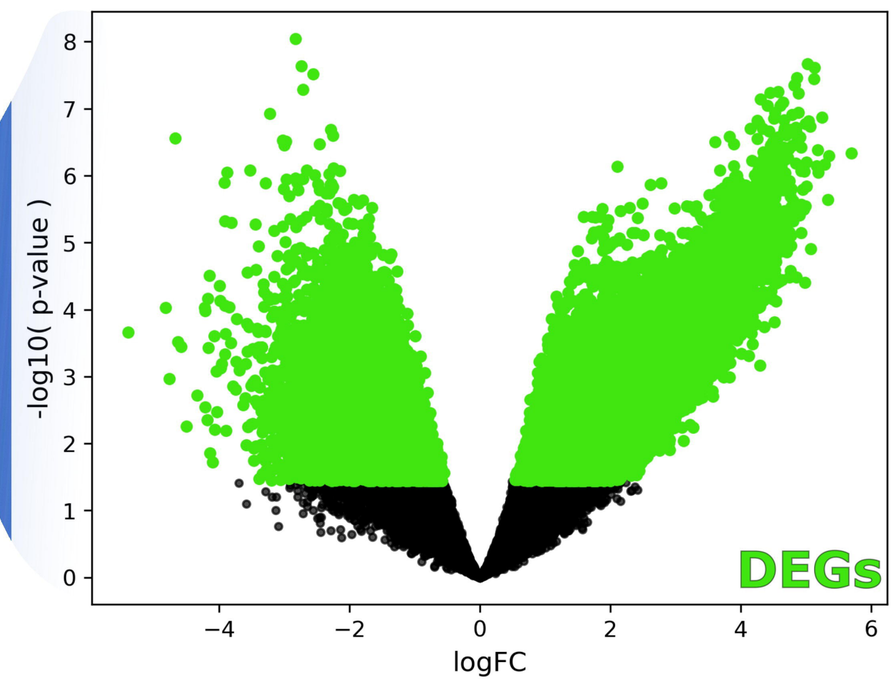
-log10(p-value)
logFC
DEGs

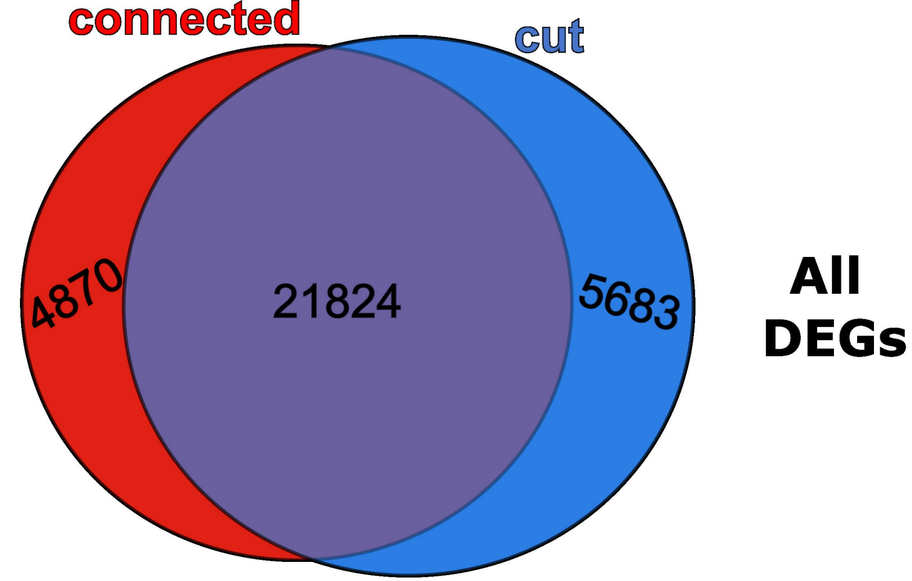
connected
cut
4870
21824
5683
All
DEGs

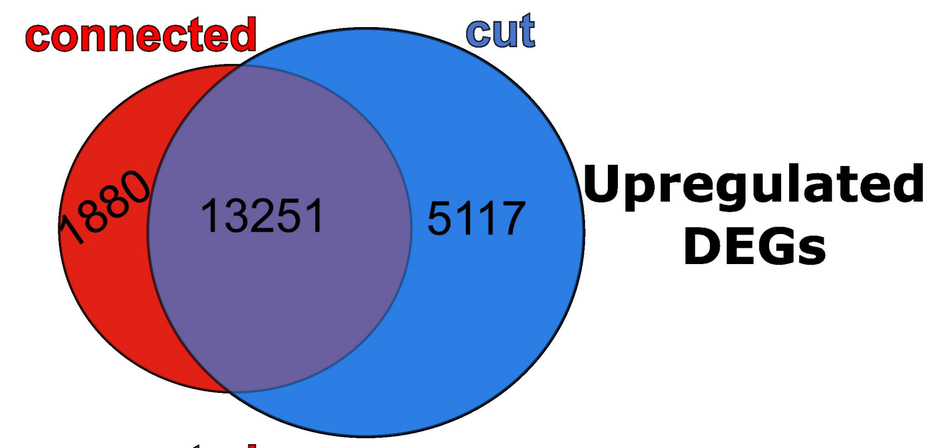
connected
cut
1880
13251
5117
Upregulated
DEGs

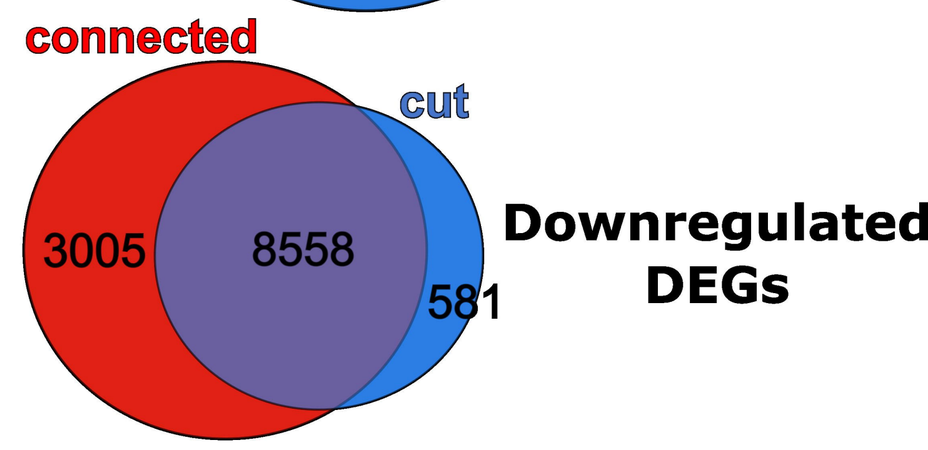
connected
cut
3005
8558
581
Downregulated
DEGs

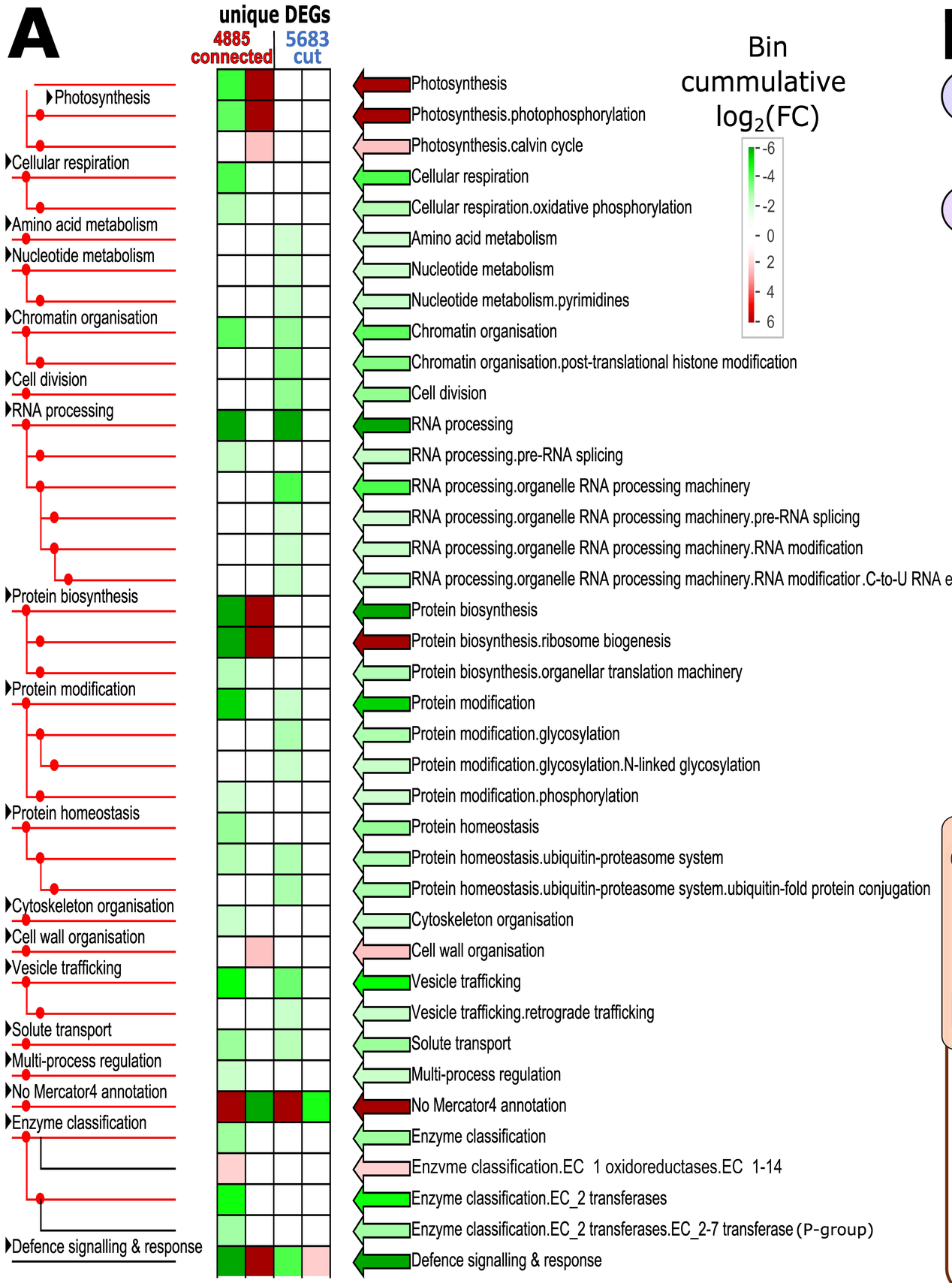
A
unique DEGs
4885 connected
5683 cut
Bin cummulative log2(FC)
-6
-4
-2
0
2
4
6
Photosynthesis
Cellular respiration
Amino acid metabolism
Nucleotide metabolism
Chromatin organisation
Cell division
RNA processing
Protein biosynthesis
Protein modification
Protein homeostasis
Cytoskeleton organisation
Cell wall organisation
Vesicle trafficking
Solute transport
Multi-process regulation
No Mercator4 annotation
Enzyme classification
Defence signalling & response
Photosynthesis
Photosynthesis.photophosphorylation
Photosynthesis.calvin cycle
Cellular respiration
Cellular respiration.oxidative phosphorylation
Amino acid metabolism
Nucleotide metabolism
Nucleotide metabolism.pyrimidines
Chromatin organisation
Chromatin organisation.post-translational histone modification
Cell division
RNA processing
RNA processing.pre-RNA splicing
RNA processing.organelle RNA processing machinery
RNA processing.organelle RNA processing machinery.pre-RNA splicing
RNA processing.organelle RNA processing machinery.RNA modification
RNA processing.organelle RNA processing machinery.RNA modificatior.C-to-U RNA editing
Protein biosynthesis
Protein biosynthesis.ribosome biogenesis
Protein biosynthesis.organellar translation machinery
Protein modification
Protein modification.glycosylation
Protein modification.glycosylation.N-linked glycosylation
Protein modification.phosphorylation
Protein homeostasis
Protein homeostasis.ubiquitin-proteasome system
Protein homeostasis.ubiquitin-proteasome system.ubiquitin-fold protein conjugation
Cytoskeleton organisation
Cell wall organisation
Vesicle trafficking
Vesicle trafficking.retrograde trafficking
Solute transport
Multi-process regulation
No Mercator4 annotation
Enzyme classification
Enzvme classification.EC 1 oxidoreductases.EC 1-14
Enzyme classification.EC_2 transferases
Enzyme classification.EC_2 transferases.EC_2-7 transferase (P-group)
Defence signalling & response

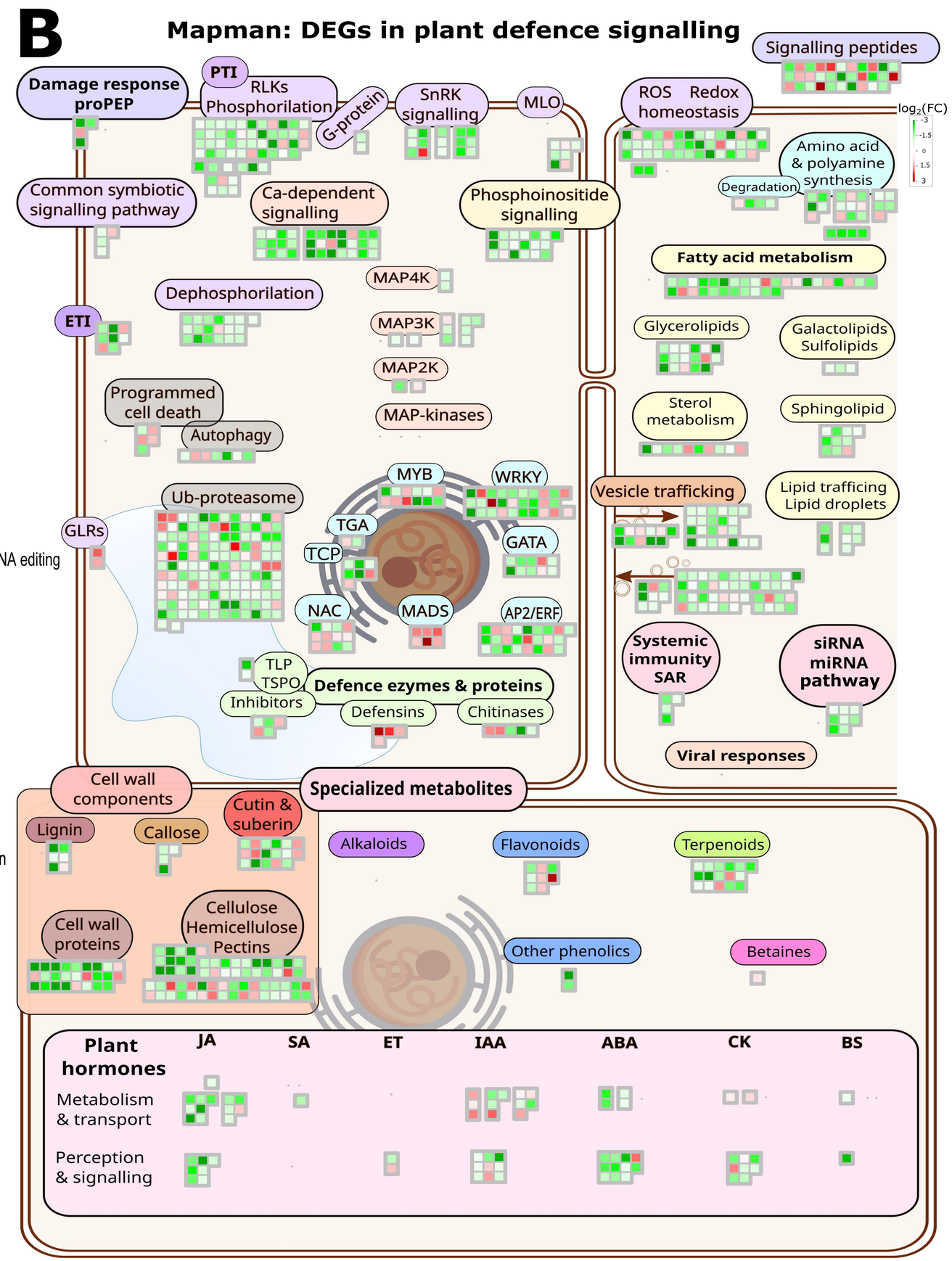
B
Mapman: DEGs in plant defence signalling
Signalling peptides
Damage response proPEP
PTI
RLKs Phosphorilation
G-protein
SnRK signalling
MLO
ROS Redox homeostasis
log2(FC)
Amino acid & polyamine synthesis
Degradation
Common symbiotic signalling pathway
Ca-dependent signalling
Phosphoinositide signalling
Fatty acid metabolism
MAP4K
Dephosphorilation
ETI
MAP3K
Glycerolipids
Galactolipids Sulfolipids
MAP2K
Programmed cell death
MAP-kinases
Sterol metabolism
Sphingolipid
Autophagy
MYB
WRKY
Vesicle trafficking
Lipid trafficking Lipid droplets
Ub-proteasome
GLRs
TGA
TCP
GATA
NAC
MADS
AP2/ERF
Systemic immunity SAR
siRNA miRNA pathway
TLP TSPO
Defence ezymes & proteins
Inhibitors
Defensins
Chitinases
Viral responses
Cell wall components
Specialized metabolites
Lignin
Callose
Cutin & suberin
Alkaloids
Flavonoids
Terpenoids
Cellulose Hemicellulose Pectins
Cell wall proteins
Other phenolics
Betaines
Plant hormones
JA
SA
ET
IAA
ABA
CK
BS
Metabolism & transport
Perception & signalling

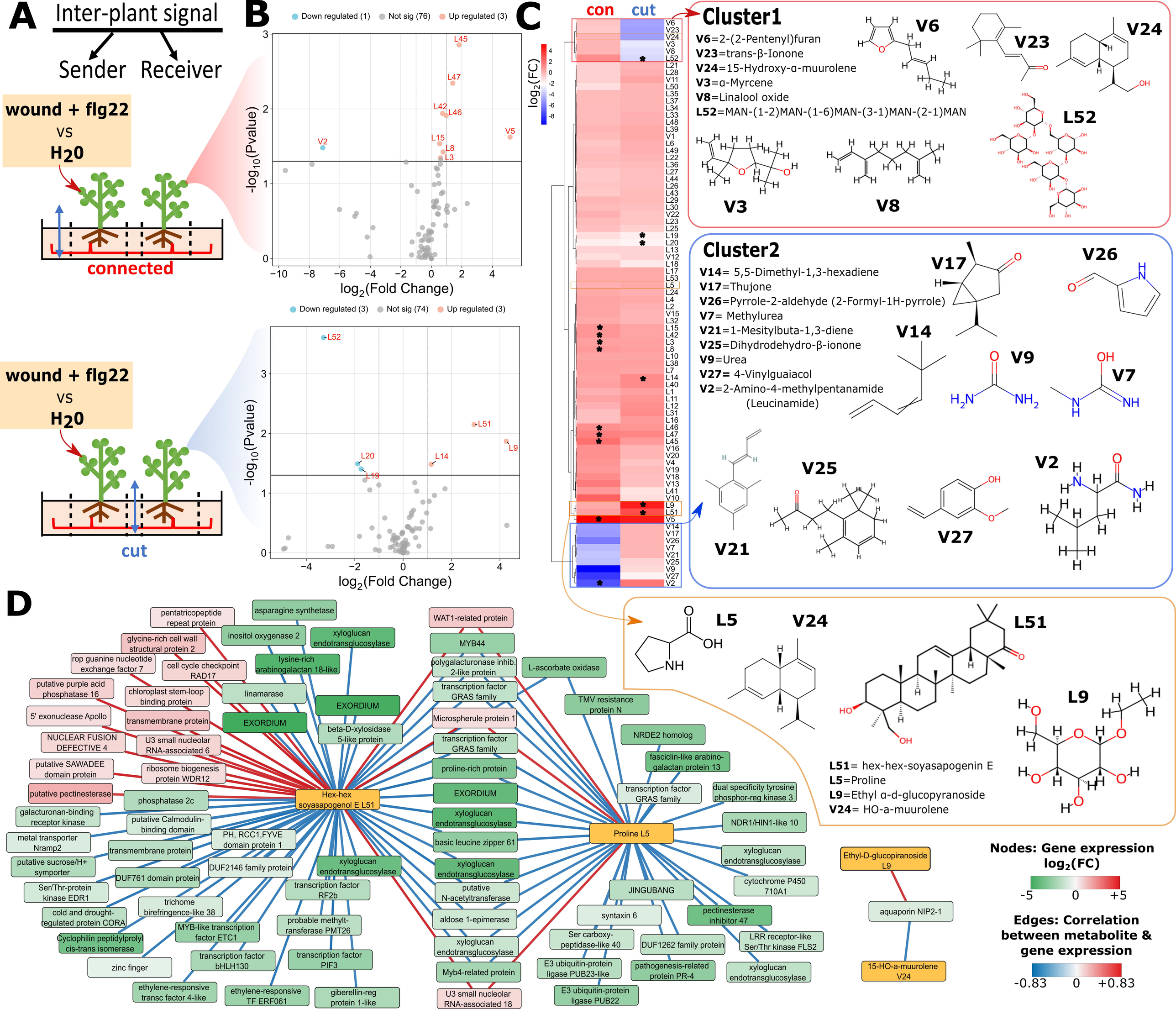
A
Inter-plant signal
Sender
Receiver
wound + flg22
vs
H20
connected
wound + flg22
vs
H20
cut
B
Down regulated (1)
Not sig (76)
Up regulated (3)
-log10(Pvalue)
log2(Fold Change)
L45
L47
L42
L46
V5
V2
L15
L8
L3
Down regulated (3)
Not sig (74)
Up regulated (3)
L52
L51
L9
L20
L19
L14
C
con
cut
log2(FC)
Cluster1
V6=2-(2-Pentenyl)furan
V23=trans-β-Ionone
V24=15-Hydroxy-α-muurolene
V3=α-Myrcene
V8=Linalool oxide
L52=MAN-(1-2)MAN-(1-6)MAN-(3-1)MAN-(2-1)MAN
V6
V23
V24
L52
V3
V8
Cluster2
V14= 5,5-Dimethyl-1,3-hexadiene
V17=Thujone
V26=Pyrrole-2-aldehyde (2-Formyl-1H-pyrrole)
V7= Methylurea
V21=1-Mesitylbuta-1,3-diene
V25=Dihydrodehydro-β-ionone
V9=Urea
V27= 4-Vinylguaiacol
V2=2-Amino-4-methylpentanamide
(Leucinamide)
V17
V26
V14
V9
V7
V25
V2
V21
V27
L5
V24
L51
L9
L51= hex-hex-soyasapogenin E
L5=Proline
L9=Ethyl α-d-glucopyranoside
V24= HO-a-muurolene
D
pentatricopeptide repeat protein
asparagine synthetase
glycine-rich cell wall structural protein 2
inositol oxygenase 2
xyloglucan endotransglucosylase
rop guanine nucleotide exchange factor 7
cell cycle checkpoint RAD17
lysine-rich arabinogalactan 18-like
putative purple acid phosphatase 16
chloroplast stem-loop binding protein
linamarase
EXORDIUM
5' exonuclease Apollo
transmembrane protein
EXORDIUM
beta-D-xylosidase 5-like protein
NUCLEAR FUSION DEFECTIVE 4
U3 small nucleolar RNA-associated 6
putative SAWADEE domain protein
ribosome biogenesis protein WDR12
putative pectinesterase
phosphatase 2c
galacturonan-binding receptor kinase
putative Calmodulin-binding domain
metal transporter Nramp2
PH, RCC1,FYVE domain protein 1
transmembrane protein
putative sucrose/H+ symporter
DUF2146 family protein
xyloglucan endotransglucosylase
DUF761 domain protein
Ser/Thr-protein kinase EDR1
transcription factor RF2b
trichome birefringence-like 38
cold and drought-regulated protein CORA
probable methyltransferase PMT26
MYB-like transcription factor ETC1
Cyclophilin peptidylprolyl cis-trans isomerase
transcription factor bHLH130
transcription factor PIF3
zinc finger
ethylene-responsive transc factor 4-like
ethylene-responsive TF ERF061
giberellin-reg protein 1-like
Hex-hex soyasapogenol E L51
WAT1-related protein
MYB44
polygalacturonase inhib. 2-like protein
L-ascorbate oxidase
transcription factor GRAS family
TMV resistance protein N
Microspherule protein 1
transcription factor GRAS family
NRDE2 homolog
proline-rich protein
fasciclin-like arabino-galactan protein 13
EXORDIUM
transcription factor GRAS family
dual specificity tyrosine phosphor-reg kinase 3
xyloglucan endotransglucosylase
NDR1/HIN1-like 10
basic leucine zipper 61
Proline L5
xyloglucan endotransglucosylase
xyloglucan endotransglucosylase
cytochrome P450 710A1
putative N-acetyltransferase
JINGUBANG
aldose 1-epimerase
syntaxin 6
pectinesterase inhibitor 47
xyloglucan endotransglucosylase
Ser carboxy-peptidase-like 40
DUF1262 family protein
LRR receptor-like Ser/Thr kinase FLS2
Myb4-related protein
E3 ubiquitin-protein ligase PUB23-like
pathogenesis-related protein PR-4
xyloglucan endotransglucosylase
U3 small nucleolar RNA-associated 18
E3 ubiquitin-protein ligase PUB22
Ethyl-D-glucopiranoside L9
aquaporin NIP2-1
15-HO-a-muurolene V24
Nodes: Gene expression log2(FC)
-5
0
+5
Edges: Correlation between metabolite & gene expression
-0.83
0
+0.83
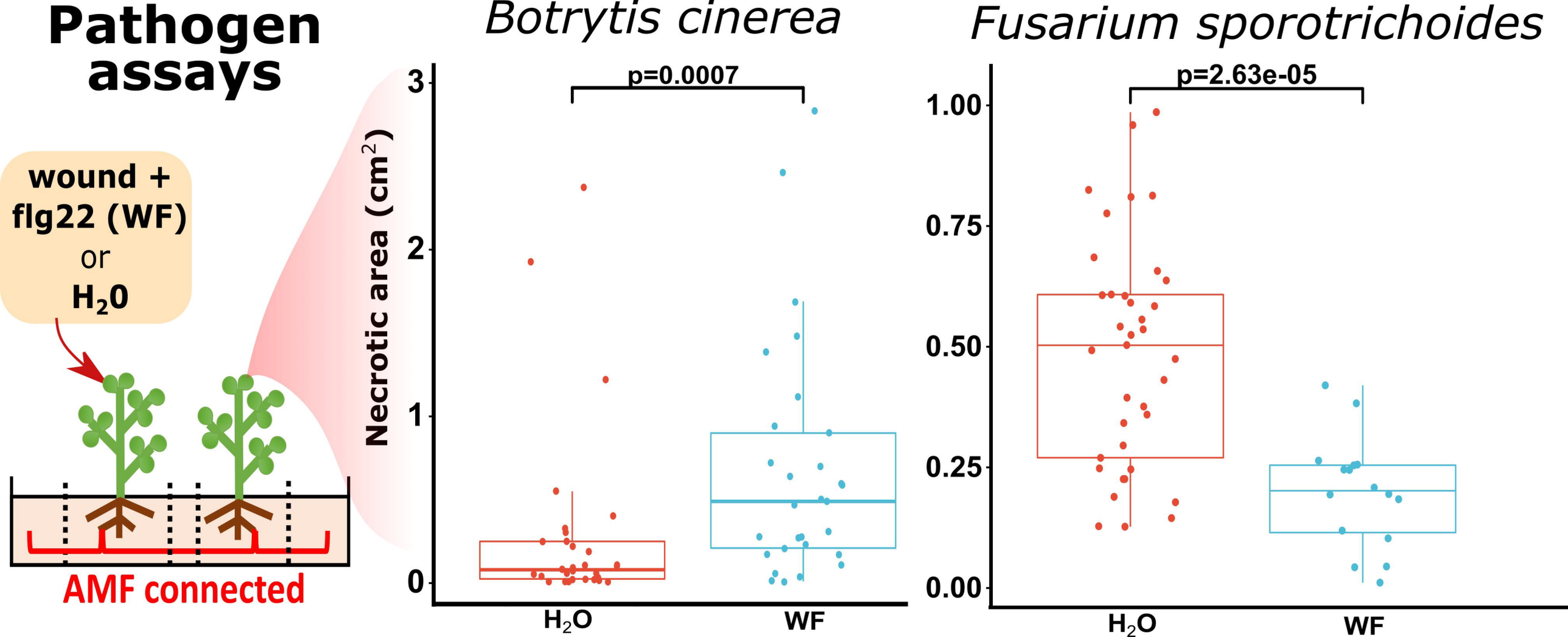
Pathogen assays